NATIONAL ADVISORY COMMITTEE FOR AERONAUTICS

TECHNICAL NOTE 3071

THEORETICAL SUPERSONIC FORCE AND MOMENT COEFFICIENTS ON A SIDESLIPPING VERTICAL- AND HORIZONTAL-TAIL COMBINATION WITH SUBSONIC LEADING EDGES AND SUPERSONIC TRAILING EDGES

By Frank S. Malvestuto, Jr.

Langley Aeronautical Laboratory
Langley Field, Va.

Washington
March 1954

1T

NATIONAL ADVISORY COMMITTEE FOR AERONAUTICS

TECHNICAL NOTE 3071

THEORETICAL SUPERSONIC FORCE AND MOMENT COEFFICIENTS ON A SIDESLIPPING VERTICAL- AND HORIZONTAL-TAIL COMBINATION WITH SUBSONIC LEADING EDGES AND SUPERSONIC TRAILING EDGES

By Frank S. Malvestuto, Jr.

SUMMARY

Theoretical expressions have been derived by means of linearized supersonic-flow theory for the lateral force due to sideslip C_{Y_β}, the yawing moment due to sideslip C_{n_β}, and the rolling moment due to sideslip C_{l_β} for tail arrangements consisting of a vertical triangular surface attached to a symmetrical triangular horizontal surface. The results are valid, in general, for a range of Mach number for which the leading edges of the tail surfaces are swept behind the Mach cone from the apex of the arrangement and the trailing edges of the tail surfaces are ahead of the Mach lines from the tips.

A series of design charts are presented which permit rapid estimates to be made of the force and moment derivatives. A discussion is also included on the application of the expressions for the pressure distributions determined herein to other plan-form shapes of the tail surfaces and possible wing—vertical-tail arrangements. A solution to a two-dimensional "mixed type" boundary-value problem which is needed in the present analysis but which may also be of interest in other "conical flow" analyses is presented in an appendix.

INTRODUCTION

The prediction of the stability of complete airplane and missile configurations requires a knowledge of the aerodynamic forces and moments acting on all the component surfaces of the airframe and the rates of change of these forces and moments with the attitude, velocity, and acceleration of the associated surfaces. The rates of change of the aerodynamic forces and moments when linearly related to the attitudes, velocities, and accelerations are commonly called stability derivatives.

Theoretical estimates of stability derivatives for a variety of wing plan forms with flat-plate cross sections are now available. Information, however, relating to the stability derivatives contributed by various nonplanar tail systems is still meager. Most of the available derivatives are for configurations composed of low-aspect-ratio surfaces (refs. 1 to 3). In reference 4, however, sideslip derivatives have been presented for tail arrangements for which all the plan-form edges are supersonic. In references 1 and 5 approximate estimates of the damping-in-roll derivatives for cruciform arrangements with high-aspect-ratio surfaces have also been reported.

The purpose of the present paper is to provide theoretical estimates of the lateral force, the rolling moment, and the yawing moment produced by the sideslipping motion of a tail arrangement consisting of a triangular vertical surface attached to a symmetrical triangular horizontal surface. The leading edges of the tail surfaces are subsonic; the trailing edges, supersonic. Consideration has also been given to the application of the results presented herein to other plan-form shapes of the tail surfaces and possible wing—vertical-tail combinations.

The analysis is performed within the framework of linearized supersonic-flow theory. Inasmuch as the linearized perturbated flow within the Mach cone from the apex of the tail is conical (the arrangement is a conical body), the analysis reduces to the solution of a singular integral equation associated with a two-dimensional "mixed type" boundary-value problem. The solution is obtained by an application of the general methods for evaluating these integral equations that have been propounded by Muskhelishvili in reference 6.

SYMBOLS

The orientation of the tail arrangement with respect to the X, Y, and Z body axes and the positive directions of the velocities, forces, and moments are indicated in figure 1.

X, Y, Z	body-axes coordinates
y_1, z_1	rectangular coordinates in plane parallel to YZ-plane
$\nu = \eta + i\zeta$	
$z = x + iy$	
$\phi(X,Y,Z)$	linearized velocity-potential function
u, v, w	X-, Y-, and Z-components of perturbation velocity, respectively (v and w are also defined in the ν-plane as being parallel to the η- and ζ-axes, respectively)

$z' = x' + iy'$

u_c, v_c, w_c	complex velocities, $u_c = u + iu^*$, $v_c = v + iv^*$, and $w_c = w + iw^*$
u^*, v^*, w^*	harmonic conjugates of the u-, v-, and w-velocities, respectively
V	free-stream velocity
M	free-stream Mach number
$B = \sqrt{M^2 - 1}$	
ρ	free-stream density
q	free-stream dynamic pressure, $\frac{1}{2}\rho V^2$
Δp	pressure difference across surface
$\Delta p/q$	pressure coefficient
α	angle of attack, radians
β	angle of sideslip, radians
c_r	common root chord of vertical and horizontal tail
$b_H/2$	semispan of horizontal tail
h	transformed semispan of horizontal tail in ν-plane
b_V	span of vertical tail
d	transformed span of vertical tail in ν-plane
x_h	transformed semispan of horizontal tail in z-plane
x_d	transformed span of vertical tail in z-plane
e_1, e_2	arbitrary real constants
S_H	area of horizontal tail
S_V	area of vertical tail

γ angle in plane of horizontal tail between a ray through origin and X-axis

γ_o angle between leading edge of horizontal tail and X-axis

$t = \tan \gamma$

$t_o = \tan \gamma_o = \frac{A_H}{4}$

ϵ angle in plane of vertical tail between a ray through origin and X-axis

ϵ_o angle between leading edge of vertical tail and X-axis

$r = \tan \epsilon$

$r_o = \tan \epsilon_o = \frac{A_V}{2}$

A_H aspect ratio of horizontal tail, $\frac{b_H^2}{S_H} = 4 \tan \gamma_o$

A_V aspect ratio of vertical tail, $\frac{b_V^2}{S_V} = 2 \tan \epsilon_o$

$$k = \frac{1 - \frac{BA_H}{4}\sqrt{\frac{B^2A_V^2}{4}\left(1 - \frac{B^2A_H^2}{16}\right) + \frac{B^2A_H^2}{16}} - \left(1 - \frac{B^2A_H^2}{16}\right)\sqrt{1 - \frac{B^2A_V^2}{4}}}{\sqrt{\frac{B^2A_V^2}{4}\left(1 - \frac{B^2A_H^2}{16}\right) + \frac{B^2A_H^2}{16}} - \frac{BA_H}{4}}$$

$cn(u/k)$, $dn(u/k)$, $sn(u/k)$ Jacobian elliptic functions of argument u and modulus k

E, E' complete elliptic integrals of second kind with moduli k and $\sqrt{1 - k^2}$, respectively

K, K' complete elliptic integrals of first kind with moduli k and $\sqrt{1 - k^2}$, respectively

$$G = \left[\frac{BA_H}{4} K'(k) + \frac{E'(k)}{k}\right] \sqrt{\frac{2k}{\sqrt{\frac{B^2A_V^2}{4}\left(1 - \frac{B^2A_H^2}{16}\right) + \frac{B^2A_H^2}{16}} - \frac{BA_H}{4}}}$$

Y lateral force, see figure 1

L' rolling moment, see figure 1

N yawing moment, see figure 1

C_Y lateral-force coefficient, $\dfrac{Y}{\frac{1}{2}\rho V^2 S_V}$

C_l rolling-moment coefficient, $\dfrac{L'}{\frac{1}{2}\rho V^2 b_V S_V}$

C_n yawing-moment coefficient, $\dfrac{N}{\frac{1}{2}\rho V^2 b_V S_V}$

$$C_{Y_\beta} = \left(\frac{\partial C_Y}{\partial \beta}\right)_{\beta \longrightarrow 0}$$

$$C_{l_\beta} = \left(\frac{\partial C_l}{\partial \beta}\right)_{\beta \longrightarrow 0}$$

$$C_{n_\beta} = \left(\frac{\partial C_n}{\partial \beta}\right)_{\beta \longrightarrow 0}$$

Subscripts:

H horizontal tail

V vertical tail

ANALYSIS

General Considerations

The object of the ensuing analysis is to determine the aerodynamic pressures and corresponding forces and moments acting on the surfaces of the tail arrangement sketched in figure 1 that are produced by the sideslipping motion of the tail. The leading edges of the horizontal and vertical surfaces are subsonic (within the Mach cone from the apex of the system) and the trailing edges are supersonic and at zero angle of sweep. It is stipulated that the tail surfaces are of zero camber and vanishingly small thickness. It is apparent that this tail configuration in sideslip attitude is equivalent (by rotation) to a right triangular wing at an angle of attack with a triangular end plate or fin at zero geometric angle of attack attached to its streamwise edge. Such an arrangement is sketched in figure 2, and for convenience this orientation of the tail arrangement is considered in the following analysis. With the orientation shown in figure 2, the surface approximately in the horizontal plane and at a constant geometric angle of attack is tentatively called the "wing" and the surface in the vertical plane and at zero geometric angle of attack is tentatively called the "fin."

The analysis is based on linearized three-dimensional supersonic-flow theory. Specifically, solutions of the linearized three-dimensional potential equation

$$B^2\phi_{XX} - \phi_{YY} - \phi_{ZZ} = 0 \tag{1}$$

are sought that satisfy certain boundary conditions associated with the wing-fin arrangement. (These boundary conditions are discussed subsequently.) Instead of equation (1), consider the following group of equations:

$$B^2u_{XX} - u_{YY} - u_{ZZ} = 0 \tag{2a}$$

$$B^2v_{XX} - v_{YY} - v_{ZZ} = 0 \tag{2b}$$

$$B^2w_{XX} - w_{YY} - w_{ZZ} = 0 \tag{2c}$$

which define the component-disturbance-velocity fields associated with the velocity potential of equation (1) and are more appropriate for the ensuing analysis. Once a proper solution to equation (1) or (2) has been obtained, the expressions for the lifting pressure may be readily determined from the linearized momentum equation

$$\frac{\Delta p}{\frac{1}{2}\rho V^2} = \frac{2}{V}\frac{\partial}{\partial X}\Delta\phi(X,Y,Z) \tag{3a}$$

or

$$\frac{\Delta p}{\frac{1}{2}\rho V^2} = \frac{2}{V}\Delta u(X,Y,Z) \tag{3b}$$

where $\Delta\phi$ is the velocity-potential difference across the surface and Δu is the corresponding longitudinal velocity difference or pressure-velocity difference across the surface. Equations (3) are consistent with the linearized theory only if the magnitudes of the perturbation velocities are equal across the lifting surface. When the magnitudes of the perturbation velocities are not equal across the lifting surface, equations (3) should contain differences in the squares of the disturbance velocities v and w. The squared terms lead to derivatives which are linear functions of α; therefore, these terms vanish because our primary interest is the evaluation of the rate of change of the aerodynamic forces and moments as α approaches zero.

Because of the conical geometry of the wing-fin arrangement, the following analysis to determine the required solution for the pressure employs the concepts of conical-flow theory. This concept implies that all disturbance-velocity quantities such as u, v, and w remain constant along rays emanating from the origin (apex of arrangement) and hence become functions of only two independent variables that specify the direction of the ray.

Busemann (ref. 7) initially showed that the assumption of conical flow implies mathematically that the disturbance-velocity field within the Mach cone of the system is governed by an elliptic differential equation, and by a transformation of coordinates this equation reduces to the two-dimensional Laplace equation with respect to either the u, v, or w perturbation velocity. The problem of obtaining a solution to equation (1) or (2) therefore reduces to one of obtaining a solution to Laplace's differential equation in two dimensions subject to certain

boundary conditions. These considerations lead naturally to a mode of solution using complex-function methods (refs. 8 to 10) and associated integral-equation concepts. The following sections present an analysis and solution of the wing-fin problem based on these procedures.

Prescribed Flow Conditions

A sketch of the wing-fin arrangement showing the body axes used in the analysis is presented in figure 3. Denoted also in this figure are the prescribed values of the disturbance velocities u, v, and w and their spatial derivatives in the plane of the wing and plane of the fin. These prescribed values of the velocities and their derivatives are determined from a knowledge of the boundary conditions, the symmetry conditions, and the equations of irrotationality.

The boundary conditions are as follows:

On the Mach cone surface,

$$u = v = w = 0$$

on the wing surface,

$$w\left(X,Y,0^{\pm}\right) = \alpha V$$

and on the fin surface,

$$v\left(X,0^{\pm},Z\right) = 0$$

From symmetry considerations (see ref. 10) it can be shown that in the plane of the wing the antisymmetric u- and v-velocities are zero off the wing. In the plane of the fin, however, the tangential velocities are not zero off the fin because the arrangement lacks symmetry with respect to the XZ-plane; in fact, these velocities must be continuous across this region.

The use in the equations of irrotationality of the given boundary values of the velocities, together with values of the velocities determined from symmetry conditions, produces the additional prescribed values of the velocity derivatives denoted in figure 3 and needed in the analysis. It is also stipulated that, as the leading edges are

approached, the disturbance velocities become locally infinite as the $-1/2$ power; that is, the flow around the subsonic leading edges behaves in the same manner as the flow around the leading edges of thin flat plates in an incompressible flow (see refs. 9 and 10). This stipulation on the type of edge singularity can be used in order to obtain a unique solution to the integral equation of the boundary-value problem that is solved subsequently (see appendix A).

Transformation of Supersonic Conical Flow to Two-Dimensional Incompressible Flow

The transformation of the supersonic conical-flow equation in u, v, or w to the two-dimensional Laplace equation was initially conceived by Busemann and expanded in concept and usefulness by many researchers, in particular, Lagerstrom, Germain, and Multhopp. Excellent discussions of the entire subject are given in the reports by these investigators (see refs. 10, 8, and 11, respectively). Only relations pertinent to the present analysis are therefore considered herein and the reader is referred to the references for proofs and detailed discussions of the relations to be presented.

Figure 4 is a sketch of an arbitrary crossflow plane in the XYZ-space. The fact that the body is conical and wholly contained within the Mach cone from the apex of the system demands that the u, v, and w disturbance velocities are homogeneous of zero order and are uniquely defined in any crossflow plane; that is, the u-, v-, and w-velocities have the functional form

$$u = u\left(\frac{Y}{X},\frac{Z}{X}\right) \qquad v = v\left(\frac{Y}{X},\frac{Z}{X}\right) \qquad w = w\left(\frac{Y}{X},\frac{Z}{X}\right)$$

Now if the X-, Y-, and Z-coordinates are transformed in the following manner:

$$\left.\begin{aligned} y_1 &= B\,\frac{Y}{X} \\ z_1 &= B\,\frac{Z}{X} \end{aligned}\right\} \tag{4}$$

then equations (2) defining the u-, v-, and w-velocities are transformed into elliptic differential equations in the two variables y_1 and z_1. Application of the nonconformal transformation (see ref. 11)

$$\nu = \eta + i\zeta = \frac{y_1}{1 - z_1^2} + i\,\frac{z_1\sqrt{1 - z_1^2 - y_1^2}}{1 - z_1^2} \tag{5}$$

transforms the u-, v-, and w-velocities from the y_1z_1-plane to the ν-plane in which each of the disturbance velocities satisfies Laplace's equation; that is, in the ν-plane,

$$\nabla^2 u = 0$$

$$\nabla^2 v = 0$$

$$\nabla^2 w = 0$$

where ∇^2 is the Laplacian operator $\left(\frac{\partial^2}{\partial\eta^2} + \frac{\partial^2}{\partial\zeta^2}\right)$. The effect of the transformation expressed by equation (5) is to deform the doubly connected annular region between the Mach cone and the body in the y_1z_1-plane (see fig. 4) into a doubly connected open-slit region in the ν-plane (see fig. 5). The continuous cut $(1,\infty,-1)$ in the ν-plane corresponds to the Mach circle in the y_1z_1-plane. If the ν-plane is considered as composed of two sheets, then the region external to the Mach circle in the y_1z_1-plane transforms into the lower sheet of the ν-surface and is connected to the upper sheet through the branch cut $(1,\infty,-1)$, that is, the transformed Mach circle. The transformation does not distort the horizontal and vertical axes, and hence the shape of the wing-fin arrangement is preserved (except for scale) in the ν-plane.

It should be pointed out that, since the wing-fin contour is transformed to one sheet (the upper sheet) of the double-sheeted ν-surface, the correspondence between the velocities in the crossflow plane of the original XYZ-system within the Mach circle and the upper sheet of the ν-surface is 1:1. Furthermore, since the transformation is conformal in the neighborhood of the η- and ζ-axes, the prescribed values of the

velocities and their spatial derivatives which are constant along the wing plane and fin plane in the original space remain constant along the η- and ζ-axes in the ν-plane.

If the complex velocities $u_c = u + iu^*$, $v_c = v + iv^*$, and $w_c = w + iw^*$ are considered in the ν-plane, then from the analysis of Hayes and Multhopp (refs. 9 and 11) the ensuing compatability relations (which take the place of the equations of continuity and irrotationality) provide the necessary relations in the ν-plane for attempted solutions:

$$dv_c = -\frac{B}{\nu} du_c \tag{6a}$$

$$dw_c = -iB \frac{\sqrt{1 - \nu^2}}{\nu} du_c \tag{6b}$$

In terms of the real parts of u_c, v_c, and w_c, the relations of equations (6) are as follows (see ref. 11):

For $\zeta = 0$ and $-1 \leqq \eta \leqq 1$,

$$\left.\begin{aligned} B \frac{\partial u}{\partial \eta} &= -\eta \frac{\partial v}{\partial \eta} \\ B \frac{\partial u}{\partial \zeta} &= -\frac{\eta}{\sqrt{1 - \eta^2}} \frac{\partial w}{\partial \eta} \\ B \frac{\partial u}{\partial \eta} &= \frac{\eta}{\sqrt{1 - \eta^2}} \frac{\partial w}{\partial \zeta} \\ \frac{\partial v}{\partial \eta} &= -\frac{1}{\sqrt{1 - \eta^2}} \frac{\partial w}{\partial \zeta} \end{aligned}\right\} \tag{7}$$

and for $\eta = 0$ and $\zeta \neq 0$,

$$\left.\begin{aligned} \frac{\partial w}{\partial \zeta} &= -B \frac{\sqrt{1 + \zeta^2}}{\zeta} \frac{\partial u}{\partial \zeta} \\ \frac{\partial v}{\partial \zeta} &= -B \frac{1}{\zeta} \frac{\partial u}{\partial \eta} \\ \frac{\partial v}{\partial \eta} &= B \frac{1}{\zeta} \frac{\partial u}{\partial \zeta} \end{aligned}\right\} \tag{8}$$

By using these relations, general solutions for the u, v, and w disturbance velocities can be determined, provided a solution exists for any one of the velocities.

Evaluation of the u Perturbation Velocity (Pressure Velocity) in the ν-Plane

The evaluation of the u perturbation velocity in the ν-plane takes on its simplest form when the complex sidewash velocity v_c along the wing-fin contour is initially determined and the u-velocity is then derived from the sidewash velocity by using equations (6) or (7). The expression for the sidewash velocity along the contour has been evaluated in appendix A by obtaining a solution to the integral equation defining the sidewash in terms of its prescribed boundary values.

In appendix A the expression for v_c is initially derived in a z-plane which is obtained conformally from the ν-plane by the following transformation:

$$z = x + iy = \pm\sqrt{\frac{\nu^2 + h^2}{1 + h^2}}$$

where the plus sign is valid for $x > 0$ and the minus sign for $x < 0$. Figure 6 is a sketch of the z-plane and shows that the wing-fin contour of the ν-plane becomes a slot along the real axis (the x-axis) of the z-plane. The details of the transformation from the ν- to the z-plane are given in appendix A. In the z-plane the expressions for the u-, v-, and w-velocities can be expressed much more compactly and simply

than in the ν-plane and for this reason many of the following solutions for the velocities are given in this plane. The expressions for the real and imaginary parts of the complex sidewash velocity along the transformed contour in the z-plane as derived in appendix A are as follows:

$$v(x,0^+) = \left(e_1 + \frac{e_2}{x}\right)\sqrt{\frac{x - x_h}{x_d - x}} \qquad \left(x_h \leqq x \leqq x_d\right) \tag{9}$$

$$v^*(x,0^+) = \left(e_1 + \frac{e_2}{x}\right)\sqrt{\frac{x_h + x}{x_d - x}} \qquad \left(-x_h \leqq x \leqq x_h\right) \tag{10}$$

where e_1 and e_2 are arbitrary real constants.

The u-velocity is immediately determined from the following relations in the ν-plane that can be determined from equations (6):

$$B\frac{\partial u}{\partial \eta} = -\eta\frac{\partial v}{\partial \eta} \qquad (-1 \leqq \eta \leqq 1; \quad \zeta = 0) \tag{11}$$

$$B\frac{\partial u}{\partial \zeta} = -\zeta\frac{\partial v^*}{\partial \zeta} \qquad (\eta = 0; \quad \zeta \geqq 0) \tag{12}$$

In the z-plane these relations become

$$B\frac{\partial u(x,0^+)}{\partial x} = -\sqrt{1 + h^2}\sqrt{x^2 - x_h{}^2}\frac{\partial v(x,0^+)}{\partial x} \qquad \left(x_h \leqq x \leqq x_d\right) \tag{13}$$

$$\left.\begin{aligned} B\frac{\partial u(x,0^+)}{\partial x} &= -\sqrt{1 + h^2}\sqrt{x_h{}^2 - x^2}\frac{\partial v^*(x,0^+)}{\partial x} \qquad \left(-x_h \leqq x \leqq 0\right) \\ B\frac{\partial u(x,0^+)}{\partial x} &= \sqrt{1 + h^2}\sqrt{x_h{}^2 - x^2}\frac{\partial v^*(x,0^+)}{\partial x} \qquad \left(0 \leqq x \leqq x_h\right) \end{aligned}\right\} \tag{14}$$

Equation (13) relates the u- and v-velocities along the transformed wing contour in the z-plane; equation (14) relates the v^*- and u-velocities along the transformed fin contour in the z-plane. Integration of equations (13) and (14), with equations (9) and (10) for v and v^* taken into account, produces the following solution for the u-velocity:

$$u(x,0^+) = -\frac{\sqrt{1+h^2}}{B}\left\{\left[e_1(x_d - x_h) + e_2\frac{x - x_h}{x}\right]\sqrt{\frac{x_h + x}{x_d - x}} - i\left[\frac{e_1}{2}(x_d - x_h) + e_2\right]\log_e \frac{x_d - x_h - 2x + 2\sqrt{(x_h + x)(x - x_d)}}{x_d + x_h} + \left[\frac{e_1}{2}(x_d - x_h) + e_2\right]\frac{\pi}{2}\right\} \qquad \left(-x_h \leqq x \leqq x_d\right) \qquad (15)$$

The relationship between e_1 and e_2 is easily determined by using equation (15) in the following manner: In the ν-plane $u(0^-,0^+)$ is known to be zero from the physical boundary conditions. Hence in the z-plane $u(x,0^+)$ is zero at $x = -x_h$. In equation (15) for the u-velocity, if x is set equal to $-x_h$ and $u(x,0^+)$ is set equal to zero, the following relation between e_1 and e_2 is obtained:

$$e_1 = \frac{2e_2}{x_h - x_d} \qquad (16)$$

The same relation between e_1 and e_2 is also obtained from the condition that the circulation along a closed path enclosing the wing-fin contour must be zero (see ref. 11). The substitution of e_1, in terms of e_2, into equation (15) yields

$$u(x,0^+) = \frac{\sqrt{1 + h^2}}{B} e_2 \left(1 + \frac{x_h}{x}\right)\sqrt{\frac{x_h + x}{x_d - x}} \qquad \left(-x_h \leqq x \leqq x_d\right) \quad (17)$$

The constant e_2 has been evaluated in appendix B and may be simply expressed as

$$e_2 = \frac{V\alpha}{\sqrt{1 + h^2}} \frac{1}{G}$$

where

$$G = \left[x_h K'(k) + \frac{E'(k)}{k}\right]\sqrt{\frac{2k}{x_d - x_h}}$$

$$k = \frac{1 - x_h x_d - \sqrt{\left(1 - x_h^2\right)\left(1 - x_d^2\right)}}{x_d - x_h}$$

In the equation for G, $K'(k)$ is the complete elliptic integral of the first kind with modulus $\sqrt{1 - k^2}$, and $E'(k)$ is the complete elliptic integral of the second kind with modulus $\sqrt{1 - k^2}$. The parameter k necessary for the determination of G may be expressed in terms of the geometric characteristics of the tail system (see appendix B). These relationships are illustrated in figure 7.

The u-velocity along the contour in the z-plane is now uniquely given as

$$u(x,0^+) = \frac{V\alpha}{BG}\left(1 + \frac{x_h}{x}\right)\sqrt{\frac{x_h + x}{x_d - x}} \quad (18)$$

The expressions for the u-velocity along the wing and fin contours in the ν-plane (see fig. 5) are easily obtained from equation (18) through the use of the transformation

$$z = x + iy = \pm\sqrt{\frac{\nu^2 + h^2}{1 + h^2}} \tag{19}$$

where, as previously stated, the plus sign is valid for $x > 0$ and the minus sign for $x < 0$. In the ν-plane the expressions for the u-velocity along the contours become:

Along the wing $(0 \leqq \eta \leqq d)$,

$$u(\eta,0^{\pm}) = \pm\frac{V\alpha}{BG}\left(1 + \frac{h}{\sqrt{\eta^2 + h^2}}\right)\sqrt{\frac{h + \sqrt{\eta^2 + h^2}}{\sqrt{d^2 + h^2} - \sqrt{\eta^2 + h^2}}} \tag{20}$$

along the upper half of the fin $(0 \leqq \zeta \leqq h)$,

$$u(\zeta,0^{\pm}) = \frac{V\alpha}{BG}\left(1 \pm \frac{h}{\sqrt{h^2 - \zeta^2}}\right)\sqrt{\frac{h \pm \sqrt{h^2 - \zeta^2}}{\sqrt{d^2 + h^2} \mp \sqrt{h^2 - \zeta^2}}} \tag{21}$$

and along the lower half of the fin $(-h \leqq \zeta \leqq 0)$,

$$u(\zeta,0^{\pm}) = \frac{V\alpha}{BG}\left(1 \mp \frac{h}{\sqrt{h^2 - \zeta^2}}\right)\sqrt{\frac{h \mp \sqrt{h^2 - \zeta^2}}{\sqrt{d^2 + h^2} \pm \sqrt{h^2 - \zeta^2}}} \tag{22}$$

The equation for u on the lower half of the fin (eq. (22)) has been obtained from equation (21) for the upper half of the fin by applying the known condition of antisymmetry of the u-velocity with respect to the η-axis.

The expressions for the pressure distributions for the wing and fin follow immediately from equations (20) to (22) through the use of the following linearized pressure-velocity relation:

$$p = -\rho V u \tag{23}$$

where p represents the disturbance pressure. The use of equation (23) yields the following expressions for the pressure coefficient for the wing and the fin:

On the wing $(0 \leqq \eta \leqq d)$,

$$\frac{\Delta p}{\frac{1}{2}\rho V^2} = \frac{p(\eta,0^-) - p(\eta,0^+)}{\frac{1}{2}\rho V^2}$$

$$= \frac{2}{V}\left[-u(\eta,0^-) + u(\eta,0^+)\right]$$

$$= \frac{4\alpha}{BG}\left(1 + \frac{h}{\sqrt{\eta^2 + h^2}}\right)\sqrt{\frac{h + \sqrt{\eta^2 + h^2}}{\sqrt{d^2 + h^2} - \sqrt{\eta^2 + h^2}}} \tag{24}$$

on the upper half of the fin $(0 \leqq \zeta \leqq h)$,

$$\frac{\Delta p}{\frac{1}{2}\rho V^2} = \frac{p(\zeta,0^-) - p(\zeta,0^+)}{\frac{1}{2}\rho V^2}$$

$$= \frac{2}{V}\left[u(\zeta,0^+) - u(\zeta,0^-)\right]$$

$$= \frac{2\alpha}{BG}\left[\left(1 + \frac{h}{\sqrt{h^2 - \zeta^2}}\right)\sqrt{\frac{h + \sqrt{h^2 - \zeta^2}}{\sqrt{d^2 + h^2} - \sqrt{h^2 - \zeta^2}}} - \right.$$

$$\left.\left(1 - \frac{h}{\sqrt{h^2 - \zeta^2}}\right)\sqrt{\frac{h - \sqrt{h^2 - \zeta^2}}{\sqrt{d^2 + h^2} + \sqrt{h^2 - \zeta^2}}}\right] \tag{25}$$

and on the lower half of the fin $(-h \leqq \zeta \leqq 0)$,

$$\frac{\Delta p}{\frac{1}{2}\rho V^2} = \frac{2\alpha}{BG}\left[\left(1 - \frac{h}{\sqrt{h^2 - \zeta^2}}\right)\sqrt{\frac{h - \sqrt{h^2 - \zeta^2}}{\sqrt{d^2 + h^2} + \sqrt{h^2 - \zeta^2}}} - \left(1 + \frac{h}{\sqrt{h^2 - \zeta^2}}\right)\sqrt{\frac{h + \sqrt{h^2 - \zeta^2}}{\sqrt{d^2 + h^2} - \sqrt{h^2 - \zeta^2}}}\right] \tag{26}$$

Evaluation of Pressure Relations for the Vertical- and Horizontal-Tail Combination in the Original Space

The results of the preceding analysis (in particular, eqs. (24) to (26)) allow the evaluation of the pressure coefficients for the wing-fin arrangement in the original XYZ-space. It is convenient, however, at this point to return to the orientation of the arrangement that is shown in figure 1 so that the wing now becomes the vertical tail and the fin the horizontal tail. It should be recalled that for convenience in the preceding analysis the tail arrangement of figure 1 was rotated to the position shown in figure 2 and the vertical tail (the lifting surface) was tentatively called the wing and the horizontal tail (the end plate) was tentatively called the fin. With this point in mind the following expressions for the pressure coefficient apply to the vertical- and horizontal-tail combination orientated as shown in figure 1 and obey the sign conventions indicated therein. The expressions for the pressure coefficients in the original XYZ-space are obtained from equations (24), (25), and (26) by the following transformation of the η,ζ variables (fig. 5) to the $\frac{Y}{X},\frac{Z}{X}$ variables by using equations (4) and (5):

In the plane of the vertical tail (or wing),

$$\eta = B\frac{Y}{X} = B \tan \epsilon = Br \tag{27}$$

$$d = B\frac{b_V}{c_r} = B \tan \epsilon_o = Br_o = \frac{BA_V}{2} \tag{28}$$

where r is the slope of a ray from the apex, b_V is the span, ϵ_o is the semiapex angle, and A_V is the aspect ratio of the vertical tail.

In the plane of the horizontal tail (or fin),

$$\zeta = \frac{B\frac{Z}{X}}{\sqrt{1 - B^2\left(\frac{Z}{X}\right)^2}} = \frac{B \tan \gamma}{\sqrt{1 - B^2\tan^2\gamma}} = \frac{Bt}{\sqrt{1 - B^2t^2}} \tag{29}$$

$$h = \frac{B\frac{b_H}{2c_r}}{\sqrt{1 - B^2\left(\frac{b_H}{2c_r}\right)^2}} = \frac{B \tan \gamma_o}{\sqrt{1 - B^2\tan^2\gamma_o}} = \frac{Bt_o}{\sqrt{1 - B^2t_o^2}} = \frac{B\frac{A_H}{4}}{\sqrt{1 - B^2\frac{A_H^2}{16}}} \tag{30}$$

where t is the slope of a ray from the apex, $b_H/2$ is the semispan, γ_o is the semivertex angle, and A_H is the aspect ratio of the horizontal tail. The substitution of equations (27) to (30) into the pressure-coefficient equations (24) to (26) results in the following relations for the pressure coefficient for the original tail arrangement in the XYZ-space of figure 1:

For the vertical tail,

$$\left(\frac{\Delta p}{\frac{1}{2}\rho V^2}\right)_V = \frac{4\beta}{BG}\left(1 + \frac{Bt_o}{\sqrt{1 - B^2t_o^2}\sqrt{B^2r^2 + \frac{B^2t_o^2}{1 - B^2t_o^2}}}\right)\sqrt{\frac{\frac{Bt_o}{\sqrt{1 - B^2t_o^2}} + \sqrt{B^2r^2 + \frac{B^2t_o^2}{1 - B^2t_o^2}}}{\sqrt{B^2r_o^2 + \frac{B^2t_o^2}{1 - B^2t_o^2}} - \sqrt{B^2r^2 + \frac{B^2t_o^2}{1 - B^2t_o^2}}}} \tag{31}$$

for the left half of the horizontal tail,

$$\left(\frac{\Delta p}{\frac{1}{2}\rho V^2}\right)_H = \frac{2\beta}{BG}\left[\left(1 + \frac{Bt_o}{\sqrt{1 - B^2t_o^2}\sqrt{\frac{B^2t_o^2}{1 - B^2t_o^2} - \frac{B^2t^2}{1 - B^2t^2}}}\right)\sqrt{\frac{\frac{Bt_o}{\sqrt{1 - B^2t_o^2}} + \sqrt{\frac{B^2t_o^2}{1 - B^2t_o^2} - \frac{B^2t^2}{1 - B^2t^2}}}{\sqrt{B^2r_o^2 + \frac{B^2t_o^2}{1 - B^2t_o^2}} - \sqrt{\frac{B^2t_o^2}{1 - B^2t_o^2} - \frac{B^2t^2}{1 - B^2t^2}}}} - \left(1 - \frac{Bt_o}{\sqrt{1 - B^2t_o^2}\sqrt{\frac{B^2t_o^2}{1 - B^2t_o^2} - \frac{B^2t^2}{1 - B^2t^2}}}\right)\sqrt{\frac{\frac{Bt_o}{\sqrt{1 - B^2t_o^2}} - \sqrt{\frac{B^2t_o^2}{1 - B^2t_o^2} - \frac{B^2t^2}{1 - B^2t^2}}}{\sqrt{B^2r_o^2 + \frac{B^2t_o^2}{1 - B^2t_o^2}} + \sqrt{\frac{B^2t_o^2}{1 - B^2t_o^2} - \frac{B^2t^2}{1 - B^2t^2}}}}\right] \tag{32}$$

and for the right half of the horizontal tail,

$$\left(\frac{\Delta p}{\frac{1}{2}\rho V^2}\right)_H = -\frac{2\beta}{BG}\left[\left(1 + \frac{Bt_o}{\sqrt{1 - B^2t_o^2}\sqrt{\frac{B^2t_o^2}{1 - B^2t_o^2} - \frac{B^2t^2}{1 - B^2t^2}}}\right)\sqrt{\frac{\frac{Bt_o}{\sqrt{1 - B^2t_o^2}} + \sqrt{\frac{B^2t_o^2}{1 - B^2t_o^2} - \frac{B^2t^2}{1 - B^2t^2}}}{\sqrt{B^2r_o^2 + \frac{B^2t_o^2}{1 - B^2t_o^2}} - \sqrt{\frac{B^2t_o^2}{1 - B^2t_o^2} - \frac{B^2t^2}{1 - B^2t^2}}}} - \left(1 - \frac{Bt_o}{\sqrt{1 - B^2t_o^2}\sqrt{\frac{B^2t_o^2}{1 - B^2t_o^2} - \frac{B^2t^2}{1 - B^2t^2}}}\right)\sqrt{\frac{\frac{Bt_o}{\sqrt{1 - B^2t_o^2}} - \sqrt{\frac{B^2t_o^2}{1 - B^2t_o^2} - \frac{B^2t^2}{1 - B^2t^2}}}{\sqrt{B^2r_o^2 + \frac{B^2t_o^2}{1 - B^2t_o^2}} + \sqrt{\frac{B^2t_o^2}{1 - B^2t_o^2} - \frac{B^2t^2}{1 - B^2t^2}}}}\right] \tag{33}$$

The parameter G appearing in these expressions may be determined from figure 8 wherein the variation of $\frac{B^2A_V^2}{4}\sqrt{\frac{16}{B^2A_H^2}-1}\,G$ with BA_V is presented for different values of BA_H. In order to facilitate estimations of G from figure 8, the variation of $\frac{B^2A_V^2}{4}\sqrt{\frac{16}{B^2A_H^2}-1}$ with BA_V for various values of BA_H is presented in figure 9.

An idea of the spanwise variation in pressure and resultant pressure for a typical vertical- and horizontal-tail combination may be obtained from figure 10. These results were obtained by use of equations (31) to (33).

It is of interest to know the expressions for the pressure coefficients for limiting cases of the tail arrangement obtained, for example, by setting the horizontal-tail span equal to zero or letting all the leading edges coincide with the Mach cone traces in the plane of the tail surfaces (sonic leading edges). Such expressions are obtained from the general expressions - equations (31) to (33) - for the pressure coefficients, provided the limiting values of the parameter G are available. The values of G for a number of limiting cases of the tail arrangement have been evaluated. These values of G, together with the corresponding expressions for the pressure coefficients, are presented in table I. It should be noted that results presented in table I for various limiting arrangements are identical to previously published results (refs. 4, 12, 13, and 14) that are available for some of these limiting arrangements.

Evaluation of Forces and Moments

The resultant aerodynamic forces and moments acting on the tail arrangement in a sideslip attitude are easily obtained by use of the pressure-coefficient expressions given by equations (31) to (33). The expressions for the resultant forces and moments to be determined obey the standard sign convention indicated in figure 1.

Lateral-force derivative C_{Y_β}.- For the tail arrangement in a positive sideslip attitude, the lateral force is defined as

$$Y = - q \iint_{S_V} \left(\frac{\Delta p}{q}\right)_V dx\, dz \tag{34}$$

where $\left(\frac{\Delta p}{q}\right)_V$ is the pressure coefficient for the vertical tail and S_V represents the vertical-tail area. The minus sign is prefixed to the integral so that the lateral force obeys the sign convention indicated in figure 1. It is clear that the horizontal tail gives a null contribution to the lateral force. The lateral-force derivative is defined as

$$C_{Y_\beta} = \left[\frac{\partial}{\partial \beta}\left(\frac{Y}{qS_V}\right)\right]_{\beta \to 0}$$

$$C_{Y_\beta} = \left\{\frac{\partial}{\partial \beta}\left[-\frac{1}{S_V}\iint_{S_V}\left(\frac{\Delta p}{q}\right)_V dx\, dz\right]\right\}_{\beta \to 0} \tag{35}$$

The substitution into equation (35) of the expression for $\left(\frac{\Delta p}{q}\right)_V$ obtained from equation (31) yields, after integration, the following expression for C_{Y_β}:

$$C_{Y_\beta} = - \frac{4\pi}{B^2 A_V G}\left(\frac{3BA_H}{\sqrt{16 - B^2A_H^2}} + \sqrt{\frac{B^2A_V^2}{4} + \frac{B^2A_H^2}{16 - B^2A_H^2}}\right) \tag{36}$$

As stated previously, estimates of the factor G can be obtained from figures 8 and 9. The variation of BC_{Y_β} with BA_V for various values of BA_H is presented in figure 11.

Rolling-moment derivative C_{l_β}.- The rolling moment produced by a positive sideslip attitude of the tail is defined as

$$L' = q\left[-\iint_{S_V}\left(\frac{\Delta p}{q}\right)_V z\,dx\,dz + \iint_{S_H}\left(\frac{\Delta p}{q}\right)_H y\,dx\,dy\right]$$

where S_H represents the horizontal-tail area. Note that the horizontal tail contributes a positive moment to the total rolling moment. The rolling-moment derivative is defined as

$$C_{l_\beta} = \left[\frac{\partial}{\partial\beta}\left(\frac{L'}{qS_Vb_V}\right)\right]_{\beta\to 0}$$

$$C_{l_\beta} = \left\{\frac{\partial}{\partial\beta}\left[-\frac{1}{S_Vb_V}\iint_{S_V}\left(\frac{\Delta p}{q}\right)_V z\,dx\,dz + \frac{1}{S_Vb_V}\iint_{S_H}\left(\frac{\Delta p}{q}\right)_H y\,dx\,dy\right]\right\}_{\beta\to 0}$$

$$C_{l_\beta} = \left(C_{l_\beta}\right)_V + \left(C_{l_\beta}\right)_H \tag{37}$$

Substituting into equation (37) the expressions for $\left(\frac{\Delta p}{q}\right)_V$ and $\left(\frac{\Delta p}{q}\right)_H$ obtained from equations (31), (32), and (33) and then performing the necessary integrations yields

$$\left(C_{l_\beta}\right)_V = -\frac{8}{3GB^3A_V^2}\left\{\left(\frac{7BA_H}{\sqrt{16 - B^2A_H^2}} + 3\sqrt{\frac{B^2A_V^2}{4} + \frac{B^2A_H^2}{16 - B^2A_H^2}}\right)\sqrt{\frac{2BA_H}{\sqrt{16 - B^2A_H^2}}\left(\sqrt{\frac{B^2A_V^2}{4} + \frac{B^2A_H^2}{16 - B^2A_H^2}} - \frac{BA_H}{\sqrt{16 - B^2A_H^2}}\right)} + \frac{3}{2}\left(\sqrt{\frac{B^2A_V^2}{4} + \frac{B^2A_H^2}{16 - B^2A_H^2}} + \frac{BA_H}{\sqrt{16 - B^2A_H^2}}\right)^2\left[\frac{\pi}{2} + \sin^{-1}\left(\frac{\sqrt{\frac{B^2A_V^2}{4} + \frac{B^2A_H^2}{16 - B^2A_H^2}} - \frac{3BA_H}{\sqrt{16 - B^2A_H^2}}}{\sqrt{\frac{B^2A_V^2}{4} + \frac{B^2A_H^2}{16 - B^2A_H^2}} + \frac{BA_H}{\sqrt{16 - B^2A_H^2}}}\right)\right]\right\} \tag{38}$$

and

$$
\begin{aligned}
\left(C_{l_\beta}\right)_H = \frac{8\left(1 - \frac{B^2A_H^2}{16}\right)}{3GB^3A_V^2} \Bigg\{ & \frac{\sqrt{1 + \frac{BA_H}{4}}\left[\sqrt{\frac{B^2A_H^2}{16}\left(1 - \frac{B^2A_V^2}{4}\right) + \frac{B^2A_V^2}{4}}\left(1 - \frac{BA_H}{2}\right) + \frac{3BA_H}{4}\right]}{2\left[1 - \sqrt{\frac{B^2A_H^2}{16}\left(1 - \frac{B^2A_V^2}{4}\right) + \frac{B^2A_V^2}{4}}\right]^{3/2}} \times \\
& \left(\frac{\pi}{2} + \tan^{-1} \left\{ \frac{\frac{\sqrt{\frac{B^2A_H^2}{16}\left(1 - \frac{B^2A_V^2}{4}\right) + \frac{B^2A_V^2}{4}}}{\frac{BA_H}{4}}\left(\frac{3BA_H}{4} + 1\right) - 3 - \frac{BA_H}{4}}{-2\sqrt{2\left[\frac{\sqrt{\frac{B^2A_H^2}{16}\left(1 - \frac{B^2A_V^2}{4}\right) + \frac{B^2A_V^2}{4}}}{\frac{BA_H}{4}} - 1\right]}\left(1 + \frac{BA_H}{4}\right)\left[1 - \sqrt{\frac{B^2A_H^2}{16}\left(1 - \frac{B^2A_V^2}{4}\right) + \frac{B^2A_V^2}{4}}\right]} \right\} \right) - \\
& \frac{\sqrt{1 - \frac{BA_H}{4}}\left[\sqrt{\frac{B^2A_H^2}{16}\left(1 - \frac{B^2A_V^2}{4}\right) + \frac{B^2A_V^2}{4}}\left(1 + \frac{BA_H}{2}\right) + \frac{3BA_H}{4}\right]}{2\left[1 + \sqrt{\frac{B^2A_H^2}{16}\left(1 - \frac{B^2A_V^2}{4}\right) + \frac{B^2A_V^2}{4}}\right]^{3/2}} \times \\
& \left(\frac{\pi}{2} + \tan^{-1} \left\{ \frac{\frac{\sqrt{\frac{B^2A_H^2}{16}\left(1 - \frac{B^2A_V^2}{4}\right) + \frac{B^2A_V^2}{4}}}{\frac{BA_H}{4}}\left(\frac{3BA_H}{4} - 1\right) + 3 - \frac{BA_H}{4}}{2\sqrt{2\left[\frac{\sqrt{\frac{B^2A_H^2}{16}\left(1 - \frac{B^2A_V^2}{4}\right) + \frac{B^2A_V^2}{4}}}{\frac{BA_H}{4}} - 1\right]}\left(1 - \frac{BA_H}{4}\right)\left[1 + \sqrt{\frac{B^2A_H^2}{16}\left(1 - \frac{B^2A_V^2}{4}\right) + \frac{B^2A_V^2}{4}}\right]} \right\} \right) - \\
& \frac{\frac{B^2A_H^2}{8}\sqrt{2\left[\frac{\sqrt{\frac{B^2A_H^2}{16}\left(1 - \frac{B^2A_V^2}{4}\right) + \frac{B^2A_V^2}{4}}}{\frac{BA_H}{4}} - 1\right]}\left[\frac{\sqrt{\frac{B^2A_H^2}{16}\left(1 - \frac{B^2A_V^2}{4}\right) + \frac{B^2A_V^2}{4}}}{\frac{BA_V}{4}}\left(1 + \frac{B^2A_H^2}{16}\right) + 2\right]}{\left(1 - \frac{B^2A_H^2}{16}\right)^2\left(1 - \frac{B^2A_V^2}{4}\right)} \Bigg\}
\end{aligned}
\tag{39}
$$

Variations of $B\left(C_{l_\beta}\right)_V$ and $B\left(C_{l_\beta}\right)_H$ with BA_V and BA_H are presented in figures 12 and 13, respectively.

Yawing-moment derivative C_{n_β}.- The yawing moment about an axis through the apex of the arrangement is given by

$$N = q \iint_{S_V} \left(\frac{\Delta p}{q}\right)_V x \, dx \, dz \tag{40}$$

(the horizontal tail offers no contribution to the yawing moment); N may also be written as

$$N = \bar{x}Y$$

where $\bar{x}$ is the x-coordinate of the point at which Y acts (often referred to as the center of pressure). An examination of the equation for $\left(\frac{\Delta p}{q}\right)_V$ (eq. (31)) shows that it is conical in form; hence, the point $\bar{x}$ will be $\frac{2}{3} c_r$ for a triangular vertical tail. This statement may be expressed in equation form as

$$\bar{x} = \frac{\iint_{S_V} \left(\frac{\Delta p}{q}\right)_V x \, dx \, dz}{\iint_{S_V} \left(\frac{\Delta p}{q}\right)_V dx \, dz} = \frac{2}{3} c_r \tag{41}$$

The yawing-moment derivative may now be simply expressed as follows:

$$C_{n_\beta} = -\frac{\frac{2}{3} c_r}{b_V} C_{Y_\beta} = -\frac{4}{3A_V} C_{Y_\beta} \tag{42}$$

or, by utilizing equation (36),

$$C_{n_\beta} = \frac{16\pi}{3B^2 A_V{}^2 G} \left(\frac{3BA_H}{\sqrt{16 - B^2 A_H{}^2}} + \sqrt{\frac{B^2 A_V{}^2}{4} + \frac{B^2 A_H{}^2}{16 - B^2 A_H{}^2}} \right) \tag{43}$$

For convenience, the variation of C_{n_β} with BA_V for a range of values of BA_H is presented in figure 14. In order to determine C_{n_β} for some other position of its moment axis, the following transfer formula is needed:

$$C_{n_\beta}' = -\left(\frac{l + \bar{x}}{b_V}\right)C_{Y_\beta} \tag{44}$$

where l is the distance parallel to the x-axis between the new position of the moment axis and the apex of the tail. Considering equation (41), equation (44) may also be written as

$$C_{n_\beta}' = -\left(\frac{l}{b_V} + \frac{4}{3A_V}\right)C_{Y_\beta} \tag{45}$$

DISCUSSION OF RESULTS

In the foregoing section general expressions for the sideslip derivatives C_{Y_β} (eq. (36)), C_{l_β} (eqs. (37) to (39)), and C_{n_β} (eq. (43)) were derived. It is of interest to present results for some limiting cases of these expressions. Table II contains analytical expressions for these derivatives for the same limiting cases of the tail arrangement that were considered for the pressure coefficients presented in table I. For the limiting case $BA_V = 2$, that is, for a vertical tail with a sonic leading edge (the Mach line coincides with the leading edge), the variation of BC_{Y_β}, BC_{l_β}, and C_{n_β} with BA_H is presented in figure 15. In a similar manner the variation of these derivatives with BA_V for $BA_H = 4$ (the leading edges of the horizontal tail are sonic) is presented in figure 16. From figure 14 the result that the yawing-moment-coefficient derivative of the vertical tail C_{n_β} is finite for $BA_V = 0$ is at first sight surprising. One would expect all derivatives to vanish when the disturbance surface (the vertical tail) vanished; however, it is to be recalled that the derivative C_{n_β} is made nondimensional with respect to $S_V b_V$ and, although the yawing moment N vanishes as $S_V \longrightarrow 0$, the ratio $N/S_V b_V$ which is in essence the coefficient remains finite since $b_V \longrightarrow 0$ as $S_V \longrightarrow 0$ and $S_V b_V$ gives an infinitesimal of the same order as N when $S_V \longrightarrow 0$.

An indication of the variation of C_{Y_β}, C_{l_β}, and C_{n_β} with Mach number for fixed aspect ratios of the vertical and horizontal tails can be obtained from figures 17, 18, and 19, respectively. The results presented in these figures for supersonic leading edges (the Mach lines behind the leading edges) were obtained from reference 4.

Although the results of the analysis presented herein are for a tail arrangement consisting of triangular horizontal and vertical surfaces, the results could be easily extended so as to include tails with sweptback or sweptforward trailing edges but of zero taper (as sketched in fig. 20), provided the angle of sweep of the trailing edges is less than the sweep angle of the Mach lines from the apex of the trailing edges (supersonic trailing edges). This limitation follows of course from the classic results of linearized flow theory that disturbances propagate only downstream and the pressure coefficients presented herein for the triangular surfaces would also be valid for sweptback or sweptforward trailing-edge surfaces with the stated limitation.

It is of interest to note that the expressions for the pressures presented in table I for the case where the leading edges of the horizontal tail are sonic are also valid for the wing--vertical-tail arrangements sketched in figure 21, provided of course it is realized that the wing must be at zero angle of attack and that the Mach lines from the apex of the vertical tail that are in the plane of the wing must intersect the trailing edge of the wing.

CONCLUDING REMARKS

Application of linearized theory has enabled an evaluation of the lateral force due to sideslip C_{Y_β}, the rolling moment due to sideslip C_{l_β}, and the yawing moment due to sideslip C_{n_β} for a tail arrangement consisting of a vertical triangular surface attached to a symmetrical horizontal triangular surface. A series of design charts have been prepared which permit rapid estimates to be made of all the derivatives for a range of Mach number for which the leading edges are subsonic and the trailing edges are supersonic.

The expressions for the pressure coefficients determined, in addition to being valid for the plan forms considered herein, are also valid for tail arrangements with sweptback or sweptforward trailing edges but of zero taper, provided the angle of sweep of the trailing edges is less than the sweep angle of the Mach lines from the apex of the trailing edges.

The expressions for the pressures also apply without change to certain wing—vertical-tail arrangements, provided the wing is at zero angle of attack and the Mach lines from the apex of the vertical tail that are in the plane of the wing intersect the trailing edge of the wing.

The solution presented for the two-dimensional "mixed type" boundary-value problem and needed in the present analysis is fundamental for problems involving vertical- and horizontal-tail combinations and is suitable for application to more complex systems than those considered herein.

Langley Aeronautical Laboratory,
National Advisory Committee for Aeronautics,
Langley Field, Va., October 16, 1953.

APPENDIX A

EVALUATION OF THE LINEARIZED DISTURBANCE VELOCITY ALONG THE CONTOUR OF THE WING-FIN ARRANGEMENT IN THE ν-PLANE

The evaluation of the tangential disturbance velocity along the wing-fin contour in the ν-plane can be performed by an application of techniques discussed by Muskhelishvili in his book on singular integral equations (ref. 6).

First, the ν-plane is conformally transformed into the z-plane by use of the transformation

$$z = x + iy = \pm\sqrt{\frac{\nu^2 + h^2}{1 + h^2}} \tag{A1}$$

where the plus sign is valid for $x > 0$ and the minus sign is valid for $x < 0$. In the z-plane (see fig. 6) the image of the wing-fin contour is a slot along the real axis (the x-axis). The branch cut $(1,\infty,-1)$ in the ν-plane representing the original Mach circle retains itself along the real axis in the z-plane.

Since the z-plane is a conformal map of the ν-plane, the complex velocities $u_c = u + iu^*$, $v_c = v + iv^*$, and $w_c = w + iw^*$ which satisfy the Laplace equation in the ν-plane also satisfy the Laplace equation in the z-plane. The given boundary values of u, v, and w and their spatial derivatives which are constants along the real and imaginary axes in the ν-plane therefore remain constant in the z-plane along the real axis.

It will be found expedient to determine the variation of v-velocity (the real part of v_c) along the wing-fin image (from $x = -x_h$ to $x = x_d$). Inasmuch as this lateral velocity is antisymmetric with respect to the η-axis in the ν-plane and the wing-fin contour is symmetric with respect to the η-axis, it is necessary to consider a solution for v in only the upper half of the ν-plane and therefore in only the upper half of the z-plane. Figure 6(b) is a sketch of the upper half of the z-plane and shows the appropriate boundary values of v and v^* along the real axis. From the boundary condition that $w = \alpha V$ on the wing, it is

possible to determine that $v^* = 0$ (or constant) along the wing segment $x_h \leqq x \leqq x_d$ in the following manner. By using equations (6a) and (6b), the relation in the ν-plane between v_c and w_c is found to be

$$dv_c = i \frac{1}{\sqrt{1 - \nu^2}} dw_c \tag{A2}$$

Along the wing axis $\nu = \eta$, and by using equation (A2) dv^* can be expressed as

$$dv^* = \frac{1}{\sqrt{1 - \eta^2}} dw \qquad (-1 \leqq \eta \leqq 1) \tag{A3}$$

Now w = Constant along the wing segment $0 \leqq \eta \leqq d$ or $dw = 0$; hence, v^* = Constant. This constant may be set equal to zero (see ref. 6). This condition $v^* = 0$ remains valid along the image of the wing segment in the z-plane.

There is one factor in the transformation of the wing-fin contour from the ν-plane to the z-plane that requires particular attention. Note that the point ih representing the leading edge of the fin in the ν-plane transforms into the origin in the z-plane and that the two faces of the fin spread out along the real axis of the z-plane, one on each side of the origin, and form a continuous segment $(-x_h, 0, x_h)$. Now if the origin is approached from above along the line $x = 0$, the v-velocity will become infinite in the immediate neighborhood of the origin even though the origin does not represent a free edge such as x_d where singularities in the boundary functions are usually allowed. This discontinuity in v follows directly from the behavior of the v-velocity in the neighborhood of the fin leading edge ih in the ν-plane. In this plane as the fin edge ih is approached from above along $i\zeta$, the v-velocity becomes a singularity of order $-1/2$; hence, in the z-plane as the origin (the image of the point ih) is approached from above along iy, the v-velocity becomes a singularity of order -1. The fact that the singularity in the v-velocity near the origin in the z-plane is of -1 order arises from the double-valuedness of the transformation from the ν-plane to the z-plane. For the subsequent analysis the point to remember from the present discussion is that the v-velocity function does not continuously approach its prescribed values for all points of the open segment $-x_h < x < x_h$ but becomes discontinuous as the origin is approached along $x = 0$. Along the remaining segments defining the wing-fin image in the z-plane, the v-velocity can be shown to approach its boundary values continuously except at free edges where singularities are of course allowed.

As indicated previously, the solution for v_c is based upon the analysis of reference 6. In order to associate the present analysis directly with the general treatise on boundary-value problems in reference 6, one additional transformation is needed; this transformation is

$$z' = \frac{2}{2z - (x_h + x_d)} \tag{A4}$$

In figure 22 the transformed wing-fin contour in the z'-plane is sketched and the corresponding boundary values of v along L' and v^* along L" are noted. It should be noted that only the upper half of the z'-plane is being considered with boundary conditions prescribed along the axis of reals. The problem at hand of determining v_c may be named the two-dimensional mixed-type boundary-value problem for the half plane.

It is well-known (see refs. 6, 8, and 11) that the solution to this type of boundary-value problem essentially involves the solution of the singular integral equation along L

$$\int_L \frac{\psi(x')}{x' - \xi} dx' = i\pi\gamma(x') \tag{A5}$$

where

$\int$ indication that the principal part of the integral is to be taken

L union of smooth nonintersecting arcs or a group of disconnected segments L' and L" along axis of reals

$\gamma(x')$ prescribed boundary function along L that must be at least continuous within the open intervals L' and L" of L ($\gamma(x')$ in the present case would correspond to prescription of $v(x')$ and $v^*(x')$ along L' and L", respectively)

$\psi(x')$ unknown function along L that is to be determined so as to be holomorphic in the region excluding L and approach on L the $\gamma(\xi)$ condition wherever prescribed ($\psi(x')$ corresponds to $v_c(x')$ in the present instance)

In reference 6, Muskhelishvili presents a thorough study of the integral equation (A5), with particular attention given to the existence and uniqueness of solutions. The case where $\gamma(x')$ is real and imaginary

along alternating segments of L (mixed-type boundary values) has received detailed attention. It is this case that is of primary interest in the present analysis for the solution of v_c along the given boundary and is now considered in detail.

Specifically, the unique function $v_c(x',0^+) = v(x',0^+) + iv^*(x',0^+)$ satisfying equation (A5) is needed; this function is to be holomorphic in the upper half plane $y' > 0$, to be bounded at infinity, and to satisfy the given boundary conditions (see figs. 22 and 23)

on L',

$$v(x',0^+) = f(x') \tag{A6a}$$

on L",

$$v^*(x',0^+) = g(x') \tag{A6b}$$

where $f(x')$ and $g(x')$ are continuous and finite along the open intervals of L' and L" and are bounded and zero at one end point of each interval but may have $-1/2$ power singularities at the other end point of these intervals. In addition, it is assumed that $g(x')$ for large values of x' is subject to the conditions

$$\lim_{x' \to \infty} g(x') = \lim_{x' \to -\infty} g(x')$$

and

$$g(x') - g(\infty) < \frac{\text{Constant}}{(x')^{\alpha}} \qquad (\alpha > 0) \tag{A7}$$

where

$$g(\infty) = \lim_{x' \to \pm\infty} g(x')$$

From the subsequent analysis it can be seen that inequality condition (A7) is satisfied in the present case. The general unique solution for v_c satisfying conditions (A6) and (A7) is given by Muskhelishvili (ref. 6, p. 253) as

$$v_c(x',0^+) = \frac{1}{\pi i}\frac{\sqrt{R_a(x')}}{\sqrt{R_b(x')}}\int_L \frac{\sqrt{R_b(\xi)}}{\sqrt{R_a(\xi)}}\frac{h(\xi)}{\xi - x'}\,d\xi + \text{Constant}\,\frac{\sqrt{R_a(x')}}{\sqrt{R_b(x')}} \qquad \text{(A8)}$$

where

$$h(\xi) = \begin{cases} f(\xi) & \text{on } L' \\ ig(\xi) & \text{on } L'' \end{cases}$$

$$R_a(\xi) = \prod_{j=1}^{p}\left(\xi - a_j\right)$$

$$R_b(\xi) = \prod_{j=1}^{p}\left(\xi - b_j\right)$$

and a_jb_j $(j = 1, 2, \ldots p)$ define the disconnected segments a_1b_1, a_2b_2, . . . along the axis of reals (see fig. 23). The application of the general solution (A8) to the particular case herein requires some additional considerations. First note that in the present instance, along L',

$$v(x',0^+) \equiv f(x',0^+) = 0 \qquad \text{(A9a)}$$

and along L'',

$$v^*(x',0^+) \equiv g(x',0^+) = 0 \qquad \text{(A9b)}$$

Now consider a modification of the given boundary-value problem in which the singularity in $v(x',0^+)$ in the neighborhood above x_o' is temporarily

neglected. For this case v approaches zero uniformly as x_o' is approached from above. With this stipulation and conditions (A9) the general solution (A8) reduces to the complementary solution (or homogeneous solution)

$$\left[\overline{v_c(x')}\right]_1 = e_1\sqrt{\frac{x' - a_1}{x' - b_1}} \tag{A10}$$

where e_1 is an arbitrary constant. The constant e_1 has been evaluated in the body of the paper (see eq. (16)).

Consider now the contribution to the solution of the singularity in v (of the order -1) as x_o' is approached from above along $x' = x_o'$. This contribution to the solution is represented by the integral term on the right-hand side of equation (A8) and can be evaluated by use of the following expediency. Assume the boundary is cut at x_o' and then displaced an infinitesimal distance 2ϵ parallel to itself; this open region is then filled in by a 2ϵ segment of the $x_o = x_o'$ line that is normal to the boundary. Now the modified boundary in the infinitesimal neighborhood of x_o' contains the singularity in v that was originally in the immediate neighborhood above x_o'. Along this modified portion of the boundary between $x_o' - \epsilon$ and $x_o' + \epsilon$ the v-function takes on the form

$$v\left(x_o' \pm \epsilon\right) = \frac{\text{Constant}}{\sqrt{\left(\xi - \alpha_1\right)\left(\alpha_2 - \xi\right)}} \tag{A11}$$

where

$$\alpha_1 = x_o' - \epsilon$$

and

$$\alpha_2 = x_o' + \epsilon$$

Equation (A11) merely represents the transformations of the original -1 singularity from the $x' = x_o'$ line to the $y_1 = 0$ line, the unit singularity redistributing itself as two -1/2 power singularities, one at

$x_o' - \epsilon$ and one at $x_o' + \epsilon$. Substituting the expression for v from equation (A11) for $h(\xi)$ in equation (A8) results in the following expression for the singularity contribution to the complex v-velocity:

$$\left[v_c(x')\right]_2 = \lim_{\epsilon \to 0} \left\{ \frac{1}{\pi i} \sqrt{\frac{x' - a_1}{x' - b_1}} \int_{\alpha_1 = x_o' - \epsilon}^{\alpha_2 = x_o' + \epsilon} \sqrt{\frac{\xi - b_1}{\xi - a_1}} \left[\frac{\text{Constant}}{\sqrt{(\xi - \alpha_1)(\alpha_2 - \xi)}} \right] \frac{d\xi}{\xi - x'} \right\} \tag{A12}$$

Application of the mean-value theorem for the prescribed infinitesimal range of integration allows equation (A12) to be more simply expressed as

$$\left[v_c(x')\right]_2 = \lim_{\epsilon \to 0} \frac{e_2'}{\pi i} \sqrt{\frac{x' - a_1}{x' - b_1}} \int_{\alpha_1 = x_o' - \epsilon}^{\alpha_2 = x_o' + \epsilon} \frac{d\xi}{(\xi - x')\sqrt{(\xi - \alpha_1)(\alpha_2 - \xi)}} \tag{A13}$$

where e_2' is an arbitrary constant and the term $\sqrt{\frac{\xi - b_1}{\xi - a_1}}$ has been made part of the constant. Integrating equation (A13) and then letting $\epsilon \longrightarrow 0$ yields

$$\left[v_c(x')\right]_2 = e_2 \frac{1}{x' - x_o'} \sqrt{\frac{x' - a_1}{x' - b_1}} \tag{A14}$$

The constant e_2 has been evaluated in appendix B.

This procedure for obtaining equation (A14) for $\left[v_c(x')\right]_2$ is by no means general; however, an evaluation of the integral of equation (A12) together with detailed considerations of the modification of the original boundary near $x' = x_o'$ (discussed previously) leads to the same expression for $\left[v_c(x')\right]_2$ that is given by equation (A14).

The complete solution for the complex v-velocity in the z'-plane is given by the sum of equations (A10) and (A14). Transforming these relations to the z-plane by use of equation (A4) yields the following equation for the v-velocity in the z-plane along the boundary $-x_h \leq x \leq x_d$:

$$v_c(x,0^+) = \left(e_1 + \frac{e_2}{x}\right)\sqrt{\frac{x - x_h}{x_d - x}} \qquad (A15)$$

The real and imaginary parts of equation (A15) correspond to equations (9) and (10) that are used in the determination of the expressions for the pressure velocity.

APPENDIX B

EVALUATION OF CONSTANT e_2

The constant e_2 may be evaluated by an integration of the w-velocity (the downwash velocity) along the η-axis in the ν-plane (fig. 5) from point d (the image of the wing leading edge) to unity (the end point of the Mach cone image). Since the w-velocity is constant (equal to αV) along the wing segment $0 \leqq \eta \leqq (d - \epsilon)_{\epsilon \longrightarrow 0}$ and equal to zero at $\eta = 1$, then the integration of the downwash between the definite limits $\eta = (d - \epsilon)_{\epsilon \longrightarrow 0}$ and $\eta = 1$ is a known quantity and the constant e_2 is readily determined.

The ensuing analysis makes use of the z-plane (fig. 6) which, as indicated in appendix A and the body of the paper, is obtained from the ν-plane by a conformal transformation. In the z-plane the downwash velocity $w(x,0^+)$ in terms of the u-velocity may be expressed as follows (see eqs. (7)):

$$w(x,0^+) = \lim_{\epsilon \longrightarrow 0} \left[-B \int_{x_d+\epsilon}^{1} \sqrt{\frac{1 - x^2}{x^2 - x_h^2}} \frac{\partial}{\partial y} u(x,0^+) dx \right] \qquad \left(x_{d+\epsilon} \leqq x \leqq 1 \right) \tag{B1}$$

The normal derivative $\frac{\partial}{\partial y} u(x,0^+)$ may be expressed in terms of the known u-velocity distribution over the wing-fin contour through the classic relation (from refs. 6 and 11)

$$\frac{\partial}{\partial y} u(x,0^+) = -\frac{1}{\pi} \frac{\partial}{\partial x} \int_{-x_h}^{x_d} \frac{u_1(x')}{x - x'} dx' \qquad \left(-x_h \leqq x' \leqq x_d; \quad x_d < x \leqq 1 \right) \tag{B2}$$

where

$$u_1(x') = \frac{\sqrt{1 + h^2}}{B} e_2 \left(1 + \frac{x_h}{x'} \right) \sqrt{\frac{x_h + x'}{x_d - x'}} \tag{B3}$$

(The functional notation $\frac{\partial}{\partial y} u(x,0^+)$ is used to indicate $\frac{\partial}{\partial y} u(x,0^+) = \lim_{y \to 0^+} \left[\frac{\partial}{\partial y} u(x,y)\right]$.) Incorporating equation (B3) into equation (B2) results in the following expression:

$$\frac{\partial}{\partial y} u(x,0^+) = -\frac{\sqrt{1 + h^2}}{\pi B} e_2 \frac{\partial}{\partial x}\left[\int_{-x_h}^{x_d} \frac{1}{x - x'} \sqrt{\frac{x_h + x'}{x_d - x'}}\, dx' + \int_{-x_h}^{x_d} \frac{x_h}{x'(x - x')} \sqrt{\frac{x_h + x'}{x_d - x'}}\, dx'\right] \qquad \begin{pmatrix} -x_h \leqq x' \leqq x_d; \\ x_d < x \leqq 1 \end{pmatrix} \quad (B4)$$

Evaluating the integrals in equation (B4) and differentiating the result with respect to x yields

$$\frac{\partial}{\partial y} u(x,0^+) = \frac{\sqrt{1 + h^2}}{B} e_2 \left[\frac{x(3x_h + x_d) - 2x_h x_d}{2x^2(x - x_d)}\right] \sqrt{\frac{x + x_h}{x - x_d}} \qquad (x_d < x \leqq 1) \quad (B5)$$

Insertion of equation (B5) for $\frac{\partial}{\partial y} u(x,0^+)$ into equation (B1) yields the following integral expression for the downwash:

$$\left[w(x,0^+)\right]_{x_d}^{1} = -\frac{\sqrt{1 + h^2}}{2} e_2 \int_{x_d}^{1} \left[-(3x_h + x_d) - \frac{x_h + x_d}{x_d x} + \frac{(x_h + x_d)(1 - x_d^2)}{x_d(x - x_d)} + \frac{2x_h}{x^2}\right] \frac{dx}{\sqrt{P(x)}} \quad (B6)$$

where

$$P(x) = (1 - x^2)(x - x_d)(x - x_h)$$

and f on the integral sign indicates that the finite part of the integral must be taken. The evaluation of the integrals of equation (B6) have been performed in appendix C. The following expression results for the downwash:

$$\left[w(x,0^+)\right]_{x_d}^{1} = e_2\sqrt{1 + h^2}\sqrt{\frac{2k}{x_d - x_h}}\left[x_h K'(k) + \frac{E'(k)}{k}\right] \tag{B7}$$

where $K'(k)$ and $E'(k)$ represent the complete elliptic integrals of the first and second kinds, respectively, each with modulus $\sqrt{1 - k^2}$. The quantity k is functionally defined as

$$k = \frac{1 - x_d x_h - \sqrt{(1 - x_h^2)(1 - x_d^2)}}{x_d - x_h} \tag{B8}$$

The downwash expression (B7) can be compactly expressed as

$$\left[w(x,0^+)\right]_{x_d}^{1} = e_2\sqrt{1 + h^2}\,G \tag{B9}$$

Then e_2 is evaluated as

$$\left[w(x,0^+)\right]_{x_d}^{1} = 0 - (-V\alpha) = V\alpha = e_2\sqrt{1 + h^2}\,G$$

$$e_2 = \frac{V\alpha}{\sqrt{1 + h^2}}\frac{1}{G} \tag{B10}$$

where G in the z-plane is defined by

$$G = \left[x_h K'(k) + \frac{E'(k)}{k}\right]\sqrt{\frac{2k}{x_d - x_h}} \tag{B11}$$

In the original space, that is, the XYZ-space (see fig. 1), the expressions for k and G become

$$k = \frac{1 - Bt_o\sqrt{B^2r_o^2\left(1 - B^2t_o^2\right) + B^2t_o^2} - \left(1 - B^2t_o^2\right)\sqrt{1 - B^2r_o^2}}{\sqrt{B^2r_o^2\left(1 - B^2t_o^2\right) + B^2t_o^2} - Bt_o} \tag{B12}$$

$$G = \sqrt{\frac{2k}{\sqrt{B^2r_o^2\left(1 - B^2t_o^2\right) + B^2t_o^2} - Bt_o}}\left[Bt_o K'(k) + \frac{E'(k)}{k}\right] \tag{B13}$$

or

$$k = \frac{1 - \frac{BA_H}{4}\sqrt{\frac{B^2A_V^2}{4}\left(1 - \frac{B^2A_H^2}{16}\right) + \frac{B^2A_H^2}{16}} - \left(1 - \frac{B^2A_H^2}{16}\right)\sqrt{1 - \frac{B^2A_V^2}{4}}}{\sqrt{\frac{B^2A_V^2}{4}\left(1 - \frac{B^2A_H^2}{16}\right) + \frac{B^2A_H^2}{16}} - \frac{BA_H}{4}} \tag{B14}$$

$$G = \sqrt{\frac{2k}{\sqrt{\frac{B^2A_V^2}{4}\left(1 - \frac{B^2A_H^2}{16}\right) + \frac{B^2A_H^2}{16}} - \frac{BA_H}{4}}}\left[\frac{BA_H}{4}K'(k) + \frac{E'(k)}{k}\right] \tag{B15}$$

The variation of k with BA_V (A_V is the aspect ratio of the vertical tail) for different values of BA_H (A_H is the aspect ratio of the horizontal tail) is presented in figure 7. Similarly, the variation of G with BA_V for various values of BA_H may be obtained from figures 8 and 9.

APPENDIX C

EVALUATION OF INTEGRALS APPEARING IN THE EXPRESSION FOR THE DOWNWASH

From appendix B the integral expression for the downwash is given by

$$\left[w(x,0^+)\right]_{x_d}^{1} = \frac{\sqrt{1+h^2}}{2} e_2 \left[(3x_h + x_d) \int_{x_d}^{1} \frac{dx}{\sqrt{(1-x^2)(x-x_d)(x-x_h)}} + \right.$$

$$\frac{x_h + x_d}{x_d} \int_{x_d}^{1} \frac{dx}{x\sqrt{(1-x^2)(x-x_d)(x-x_h)}} - 2x_h \int_{x_d}^{1} \frac{dx}{x^2\sqrt{(1-x^2)(x-x_d)(x-x_h)}} -$$

$$\left. \frac{(x_h + x_d)(1-x_d^2)}{x_d} f\int_{x_d}^{1} \frac{dx}{(x-x_d)^{3/2}\sqrt{(1-x^2)(x-x_h)}} \right] \tag{C1}$$

The index f indicates that the finite part of the integral must be taken. The integrals appearing on the right-hand side of equation (C1) are essentially elliptic and can be transformed into the standard form (plus elementary integrals) by use of the linear transformation

$$\tau = \frac{1 + \dfrac{k - x_d}{1 - kx_d} x}{\dfrac{k - x_d}{1 - kx_d} + x} \tag{C2}$$

The transforms for x_d and x_h are

$$\left.\begin{aligned} x_d &= \frac{2k + k^2 x_h + x_h}{k^2 + 2kx_h + 1} \\ x_h &= \frac{-2k + k^2 x_d + x_d}{k^2 - 2kx_d + 1} \end{aligned}\right\} \tag{C3}$$

where

$$k = \frac{1 - x_h x_d - \sqrt{\left(1 - x_h^2\right)\left(1 - x_d^2\right)}}{x_d - x_h}$$

Substitution of equations (C2) and (C3) into the downwash expression, equation (C1), yields

$$\left[w(\tau,0^+)\right]_{1/k}^{1} = \frac{\sqrt{1 + h^2}}{2} e_2 \sqrt{\frac{2k}{x_d - x_h}} \left\{ \frac{(x_h + x_d)(1 - k^2)}{k(k - x_d)} \int_{1/k}^{1} \frac{d\tau}{\sqrt{(\tau^2 - 1)(1 - k^2\tau^2)}} - \right.$$

$$\frac{i(x_h + x_d)(1 - k^2)}{x_d k^3} \int_{1/k}^{1} \frac{\tau\, d\tau}{\left(\tau^2 - \frac{1}{k^2}\right)^{3/2}\sqrt{\tau^2 - 1}} - \frac{i(x_h + x_d)(1 - k^2)}{x_d k^4} \int_{1/k}^{1} \frac{d\tau}{\left(\tau^2 - \frac{1}{k^2}\right)^{3/2}\sqrt{\tau^2 - 1}} +$$

$$\left. \frac{2\left(1 - x_d^2\right)}{x_d\left(k^2 - 2x_d k + 1\right)} \int_{1/k}^{1} \sqrt{\frac{1 - k^2\tau^2}{\tau^2 - 1}}\, d\tau \right\} \qquad \text{(C4)}$$

It is obvious from inspection that equation (C4) can be written in a more compact form; however, the presented form of equation (C4) is appropriate for rapid examination of limiting cases of the wing-fin arrangement (for example, when $x_h = 0$, that is, when the fin disappears, the corresponding downwash integral is readily ascertained). The integrals appearing in equation (C4) are readily evaluated with the aid of the following substitutions:

$$\left.\begin{aligned} \tau &= \operatorname{sn}(u/k) \\ \sqrt{1 - \tau^2} &= \operatorname{cn}(u/k) \\ \sqrt{1 - \tau^2 k^2} &= \operatorname{dn}(u/k) \end{aligned}\right\} \qquad \text{(C5)}$$

where $sn(u/k)$, $cn(u/k)$, and $dn(u/k)$ represent the Jacobian elliptic functions of argument u and modulus k. The evaluation of the integrals is as follows:

$$\int_{1/k}^{1} \frac{d\tau}{\sqrt{(1 - k^2\tau^2)(\tau^2 - 1)}} = \int_{K+iK'}^{K} \frac{du}{i} = -\frac{iK'(k)}{i} = -K'(k)$$

$$\int_{1/k}^{1} \sqrt{\frac{1 - k^2\tau^2}{\tau^2 - 1}}\, d\tau = \frac{1}{i} \int_{K+iK'}^{K} dn^2u\, du = E'(k) - K'(k)$$

In order to evaluate the finite parts of the integrals

$$\int_{1/k}^{1} \frac{d\tau}{\left(\tau^2 - \frac{1}{k^2}\right)^{3/2}\sqrt{\tau^2 - 1}} \quad \text{and} \quad \int_{1/k}^{1} \frac{\tau\, d\tau}{\left(\tau^2 - \frac{1}{k^2}\right)^{3/2}\sqrt{\tau^2 - 1}}$$

the following relation for the finite part was found most convenient:

$$f\int_{a}^{b} \frac{A(\tau)d\tau}{(\tau^2 - a^2)^{3/2}} = \int_{a}^{b} \frac{A(\tau) - A(a)}{(\tau^2 - a^2)^{3/2}}\, d\tau - \frac{bA(a)}{a^2\sqrt{b^2 - a^2}} \tag{C6}$$

where $A(\tau)$ is an integrable function in the closed interval ab. Studies of finite-part concepts are presented in references 15 and 16.

Application of equation (C6) results in the following evaluations of the preceding integrals:

$$f\int_{1/k}^{1} \frac{d\tau}{\left(\tau^2 - \frac{1}{k^2}\right)^{3/2}\sqrt{\tau^2 - 1}} = \int_{1/k}^{1} \frac{d\tau}{\left(\tau^2 - \frac{1}{k^2}\right)^{3/2}\sqrt{\tau^2 - 1}} - \frac{k^4}{k'}\int_{1/k}^{1} \frac{d\tau}{\left(\tau^2 k^2 - 1\right)^{3/2}} - \frac{k^4}{ik'^2}$$

$$= k^3 \int_{K+iK'}^{K} \frac{du}{dn^2 u} + \frac{k^4}{ik'}\int_{K+iK'}^{K} \frac{cnu}{dn^2 u}\,du - \frac{k^4}{ik'^2}$$

$$= \frac{ik^3}{k'^2}\left[E'(k) - K'(k)\right]$$

$$f\int_{1/k}^{1} \frac{\tau\,d\tau}{\left(\tau^2 - \frac{1}{k^2}\right)^{3/2}\sqrt{\tau^2 - 1}} = \int_{1/k}^{1} \frac{\tau\,d\tau}{\left(\tau^2 - \frac{1}{k^2}\right)^{3/2}\sqrt{\tau^2 - 1}} - \frac{1}{k'}\int_{1/k}^{1} \frac{d\tau}{\left(\tau^2 - \frac{1}{k^2}\right)^{3/2}} - \frac{k^3}{ik'^2}$$

$$= 0$$

REFERENCES

1. Ribner, Herbert S.: Damping in Roll of Cruciform and Some Related Delta Wings at Supersonic Speeds. NACA TN 2285, 1951.

2. Bobbitt, Percy J., and Malvestuto, Frank S., Jr.: Estimation of Forces and Moments Due to Rolling for Several Slender-Tail Configurations at Supersonic Speeds. NACA TN 2955, 1953.

3. Adams, Gaynor J., and Dugan, Duane W.: Theoretical Damping in Roll and Rolling Moment Due to Differential Wing Incidence for Slender Cruciform Wings and Wing-Body Combinations. NACA Rep. 1088, 1952.

4. Martin, John C., and Malvestuto, Frank S., Jr.: Theoretical Force and Moments Due to Sideslip of a Number of Vertical Tail Configurations at Supersonic Speeds. NACA TN 2412, 1951.

5. Bleviss, Zegmund O.: Some Roll Characteristics of Cruciform Delta Wings at Supersonic Speeds. Jour. Aero. Sci., vol. 18, no. 5, May 1951, pp. 289-297.

6. Muskhelishvili, N. I.: Singular Integral Equations. Boundary Problems of Function Theory and Their Application to Mathematical Physics (Second ed., 1946). Translation No. 12, Aero. Res. Labs., Dept. Supply and Dev., Commonwealth of Australia, Feb. 1949.

7. Busemann, Adolf: Infinitesimal Conical Supersonic Flow. NACA TM 1100, 1947.

8. Germain, Paul: La Théorie générale des mouvements coniques et ses applications a l'aérodynamique supersonique. O.N.E.R.A. Publication No. 34, 1949.

9. Hayes, Wallace D.: Linearized Supersonic Flow. Rep. No. AL-222, North American Aviation, Inc., June 18, 1947.

10. Lagerstrom, P. A.: Linearized Supersonic Theory of Conical Wings. NACA TN 1685 (Corrected copy), 1950.

11. Multhopp, H.: A Unified Theory of Supersonic Wing Flow, Employing Conical Fields. Rep. No. Aero. 2415, British R.A.E., Apr. 1951.

12. Katzoff, S., and Mutterperl, William: The End-Plate Effect of a Horizontal-Tail Surface on a Vertical-Tail Surface. NACA TN 797, 1941.

13. Heaslet, Max. A., Lomax, Harvard, and Jones, Arthur L.: Volterra's Solution of the Wave Equation as Applied to Three-Dimensional Supersonic Airfoil Problems. NACA Rep. 889, 1947. (Supersedes NACA TN 1412.)

14. Brown, Clinton E.: Theoretical Lift and Drag of Thin Triangular Wings at Supersonic Speeds. NACA Rep. 839, 1946. (Supersedes NACA TN 1183.)

15. Hadamard, Jacques: Lectures on Cauchy's Problem in Linear Partial Differential Equations. Yale Univ. Press (New Haven), 1923.

16. Heaslet, Max. A., and Lomax, Harvard: The Use of Source-Sink and Doublet Distributions Extended to the Solution of Boundary-Value Problems in Supersonic Flow. NACA Rep. 900, 1948. (Supersedes NACA TN 1515.)

TABLE I.- SUMMARY OF PRESSURE COEFFICIENTS FOR VARIOUS LIMITING CASES OF THE GENERAL TAIL ARRANGEMENT SHOWN IN FIGURE 1

Limiting conditions	Pressure coefficient	Remarks
Slender tail $(A_H \to 0;\ A_V \to 0)$		
$\lim_{\substack{A_V \to 0 \\ A_H \to 0}} G = \infty$ or $\left(\frac{B^2 r_o^2}{Bt_o}\sqrt{1 - B^2 t_o^2}\right) G =$ $\left(\frac{B^2 A_V^2}{4}\sqrt{\frac{16}{B^2 A_H^2} - 1}\right) G = 4$	$\left(\frac{\Delta p}{q}\right)_V = \frac{4\beta}{BG}\left(1 + \frac{t_o}{\sqrt{r^2 + t_o^2}}\right)\sqrt{\frac{t_o + \sqrt{r^2 + t_o^2}}{\sqrt{r_o^2 + t_o^2} - \sqrt{r^2 + t_o^2}}}$	
	$*\left(\frac{\Delta p}{q}\right)_H = -\frac{2\beta}{BG}\left[\left(1 + \frac{t_o}{\sqrt{t_o^2 - t^2}}\right)\sqrt{\frac{t_o + \sqrt{t_o^2 - t^2}}{\sqrt{r_o^2 + t_o^2} - \sqrt{r^2 + t_o^2}}} - \left(1 - \frac{t_o}{\sqrt{t_o^2 - t^2}}\right)\sqrt{\frac{t_o - \sqrt{t_o^2 - t^2}}{\sqrt{r_o^2 + t_o^2} + \sqrt{t_o^2 - t^2}}}\right]$	Evaluated in ref. 12
Vertical tail alone $(A_H = 0;\ 0 \leq BA_V \leq 2)$		
$**G = \sqrt{\frac{2}{1 - \sqrt{1 - B^2 r_o^2}}}\,E'(k)$ $= \sqrt{\frac{2}{1 - \sqrt{1 - \frac{B^2 A_V^2}{4}}}}\,E'(k)$	$\left(\frac{\Delta p}{q}\right)_V = \frac{4\beta}{BG}\sqrt{\frac{r}{r_o - r}}$	Evaluated in ref. 13
Leading edge of vertical tail sonic $(BA_V = 2;\ 0 \leq BA_H \leq 4)$		
$G = \sqrt{\frac{2}{1 - Bt_o}}\,\frac{\pi}{2}\left(1 + Bt_o\right)$ $= \sqrt{\frac{2}{1 - \frac{BA_H}{4}}}\,\frac{\pi}{2}\left(1 + \frac{BA_H}{4}\right)$	$\left(\frac{\Delta p}{q}\right)_V = \frac{4\beta}{BG}\left[1 + \frac{t_o}{\sqrt{r^2(1 - B^2 t_o^2) + t_o^2}}\right]\sqrt{\frac{Bt_o + \sqrt{B^2 r^2(1 - B^2 t_o^2) + B^2 t_o^2}}{1 - \sqrt{B^2 r^2(1 - B^2 t_o^2) + B^2 t_o^2}}}$	
	$*\left(\frac{\Delta p}{q}\right)_H = -\frac{2\beta}{BG}\left[\left(1 + \frac{Bt_o}{\sqrt{1 - B^2 t_o^2}\sqrt{\frac{B^2 t_o^2}{1 - B^2 t_o^2} - \frac{B^2 t^2}{1 - B^2 t^2}}}\right) \times \sqrt{\frac{\frac{Bt_o}{\sqrt{1 - B^2 t_o^2}} + \sqrt{\frac{B^2 t_o^2}{1 - B^2 t_o^2} - \frac{B^2 t^2}{1 - B^2 t^2}}}{\sqrt{1 + \frac{B^2 t_o^2}{1 - B^2 t_o^2}} - \sqrt{\frac{B^2 t_o^2}{1 - B^2 t_o^2} - \frac{B^2 t^2}{1 - B^2 t^2}}}} - \left(1 - \frac{Bt_o}{\sqrt{1 - B^2 t_o^2}\sqrt{\frac{B^2 t_o^2}{1 - B^2 t_o^2} - \frac{B^2 t^2}{1 - B^2 t^2}}}\right)\sqrt{\frac{\frac{Bt_o}{\sqrt{1 - B^2 t_o^2}} - \sqrt{\frac{B^2 t_o^2}{1 - B^2 t_o^2} - \frac{B^2 t^2}{1 - B^2 t^2}}}{\sqrt{1 + \frac{B^2 t_o^2}{1 - B^2 t_o^2}} + \sqrt{\frac{B^2 t_o^2}{1 - B^2 t_o^2} - \frac{B^2 t^2}{1 - B^2 t^2}}}}\right]$	
Leading edge of horizontal tail sonic $(BA_H = 4;\ 0 \leq BA_V \leq 2)$		
$\lim_{BA_H \to 4} G = \infty$ or $\left(\frac{B^2 r_o^2}{Bt_o}\sqrt{1 - B^2 t_o^2}\right) G =$ $\left(\frac{B^2 A_V^2}{4}\sqrt{\frac{16}{B^2 A_H^2} - 1}\right) G =$ $4E'(Br_o) = 4E'\left(\frac{BA_V}{2}\right)$	$\left(\frac{\Delta p}{q}\right)_V = \frac{1}{G}\frac{16\beta t_o}{B\sqrt{1 - B^2 t_o^2}\sqrt{r_o^2 - r^2}}$	Corresponds to pressure loading on one panel of symmetrical triangular wing; evaluated in ref. 14
	$*\left(\frac{\Delta p}{q}\right)_H = -\frac{1}{G}\frac{8\beta t_o}{B\sqrt{1 - B^2 t_o^2}}\sqrt{\frac{1 - B^2 t^2}{t^2(1 - B^2 r_o^2) + r_o^2}}$	
Leading edges of horizontal and vertical tails sonic $(BA_V = 2;\ BA_H = 4)$		
$\lim_{\substack{BA_V \to 2 \\ BA_H \to 4}} G = \infty$ or $\left(\frac{B^2 r_o^2}{Bt_o}\sqrt{1 - B^2 t_o^2}\right) G =$ $\left(\frac{B^2 A_V^2}{4}\sqrt{\frac{16}{B^2 A_H^2} - 1}\right) G = 2\pi$	$\left(\frac{\Delta p}{q}\right)_V = \frac{1}{G}\frac{16\beta}{B\left(\frac{B^2 r_o^2}{Bt_o}\sqrt{1 - B^2 t_o^2}\right)\sqrt{1 - B^2 r^2}}$	Evaluated in refs. 14 and 4
	$*\left(\frac{\Delta p}{q}\right)_H = -\frac{1}{G}\frac{8\beta}{B\left(\frac{B^2 r_o^2}{Bt_o}\sqrt{1 - B^2 t_o^2}\right)}\sqrt{1 - B^2 t^2}$	Evaluated in ref. 4

*For the horizontal tail, pressure coefficients are presented only for the right panel.

** $k = \dfrac{1 - \sqrt{1 - \frac{B^2 A_V^2}{4}}}{\frac{BA_V}{2}}$.

TABLE II.- SUMMARY OF SIDESLIP DERIVATIVES FOR VARIOUS LIMITING CASES OF THE GENERAL TAIL ARRANGEMENT SHOWN IN FIGURE 1

Derivative	Remarks
Slender tail $(A_H \longrightarrow 0;\ A_V \longrightarrow 0)$	
$C_{Y_\beta} = -\frac{\pi A_V}{2A_H}\left(\frac{3A_H}{2} + \sqrt{A_V^2 + \frac{A_H^2}{4}}\right)$	Evaluated in ref. 12
$C_{n_\beta} = \frac{2\pi}{3A_H}\left(\frac{3A_H}{2} + \sqrt{A_V^2 + \frac{A_H^2}{4}}\right)$	
$\left(C_{l_\beta}\right)_V = -\frac{1}{3A_H}\left\{\left(\frac{7A_H}{4} + \frac{3}{2}\sqrt{A_V^2 + \frac{A_H^2}{4}}\right)\sqrt{A_H\left(\sqrt{A_V^2 + \frac{A_H^2}{4}} - \frac{A_H}{2}\right)} + \frac{3}{4}\left(\sqrt{A_V^2 + \frac{A_H^2}{4}} + \frac{A_H}{2}\right)^2\left[\frac{\pi}{2} + \sin^{-1}\left(\frac{\sqrt{A_V^2 + \frac{A_H^2}{4}} - \frac{3A_H}{2}}{\sqrt{A_V^2 + \frac{A_H^2}{4}} + \frac{A_H}{2}}\right)\right]\right\}$	
Vertical tail alone $(A_H = 0;\ 0 \leqq BA_V \leqq 2)$	
$C_{Y_\beta} = -\frac{\pi\sqrt{2}\sqrt{1 - \sqrt{1 - \frac{B^2A_V^2}{4}}}}{BE'(k)}$	Evaluated in ref. 13
$*C_{n_\beta} = \frac{4\pi\sqrt{2}\sqrt{1 - \sqrt{1 - \frac{B^2A_V^2}{4}}}}{3E'(k)BA_V}$	
$\left(C_{l_\beta}\right)_V = -\frac{\pi\sqrt{1 - \sqrt{1 - \frac{B^2A_V^2}{4}}}}{\sqrt{2}BE'(k)}$	
Leading edge of vertical tail sonic $(BA_V = 2;\ 0 \leqq BA_H \leqq 4)$	
$C_{Y_\beta} = -\frac{4\sqrt{2}(3BA_H + 4)}{B(4 + BA_H)^{3/2}}$	
$C_{n_\beta} = \frac{8\sqrt{2}(3BA_H + 4)}{3(4 + BA_H)^{3/2}}$	
$\left(C_{l_\beta}\right)_V = \frac{-4\sqrt{2}}{3B\pi\sqrt{4 - BA_H(4 + BA_H)}^2}\left\{(7BA_H + 12)\sqrt{2BA_H(4 - BA_H)} + \frac{3}{2}(4 + BA_H)^2\left[\frac{\pi}{2} + \sin^{-1}\left(\frac{4 - 3BA_H}{4 + BA_H}\right)\right]\right\}$	
Leading edge of horizontal tail sonic $(BA_H = 4;\ 0 \leqq BA_V \leqq 2)$	
$C_{Y_\beta} = -\frac{\pi A_V}{E'\left(\frac{BA_V}{2}\right)}$	Evaluated in ref. 14
$C_{n_\beta} = \frac{4\pi}{3E'\left(\frac{BA_V}{2}\right)}$	
$\left(C_{l_\beta}\right)_V = -\frac{4A_V}{3E'\left(\frac{BA_V}{2}\right)}$	
Leading edges of horizontal and vertical tails sonic $(BA_V = 2;\ BA_H = 4)$	
$C_{Y_\beta} = -\frac{4}{B}$ $\quad C_{n_\beta} = \frac{8}{3}$ $\quad \left(C_{l_\beta}\right)_V = -\frac{16}{3\pi B}$ $\quad \left(C_{l_\beta}\right)_H = \frac{16}{9\pi B}$	Can be evaluated from ref. 4

* $k = \dfrac{1 - \sqrt{1 - \frac{B^2A_V^2}{4}}}{\frac{BA_V}{2}}$.

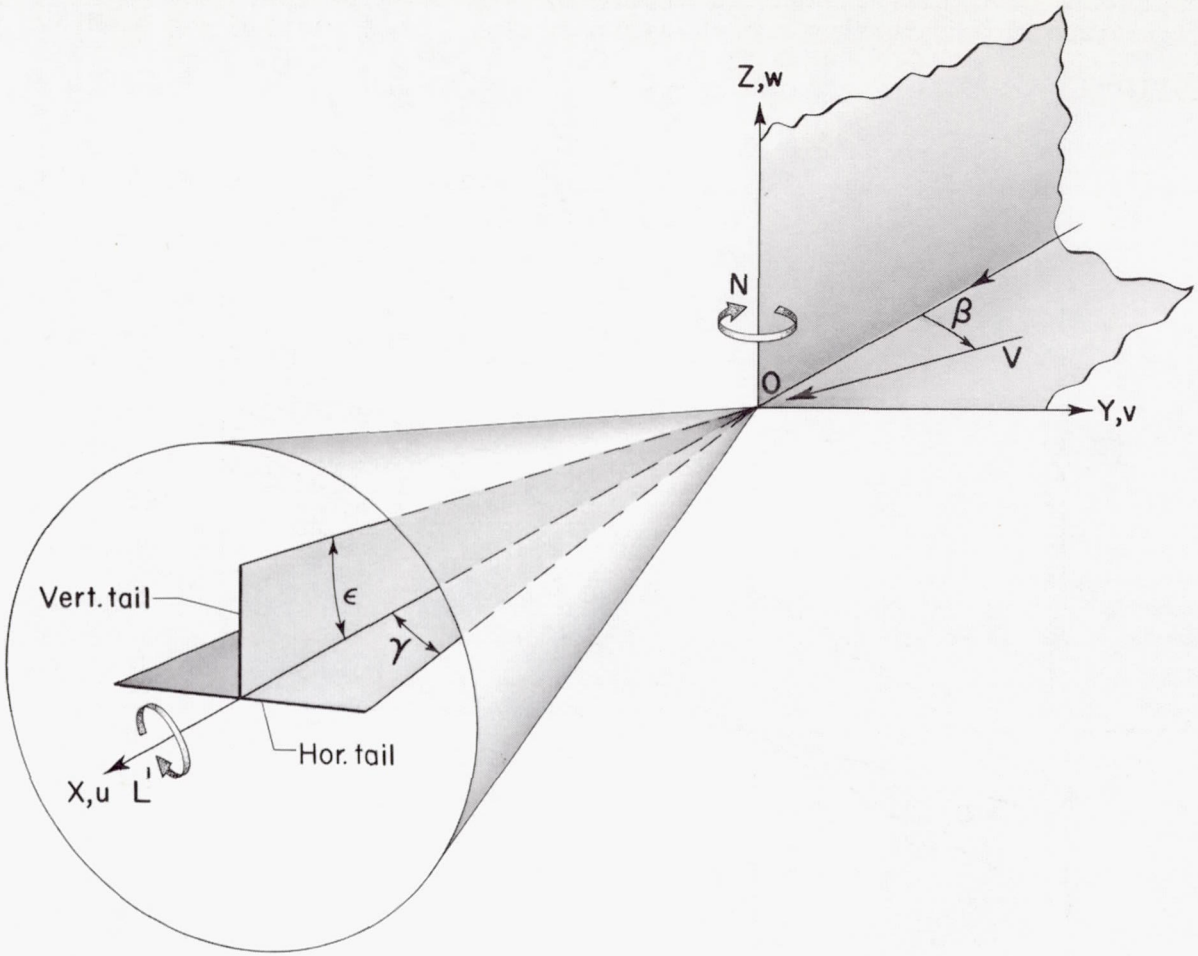

L-81261

Figure 1.- Sketch of tail arrangement showing positive directions of velocities, forces, and moments.

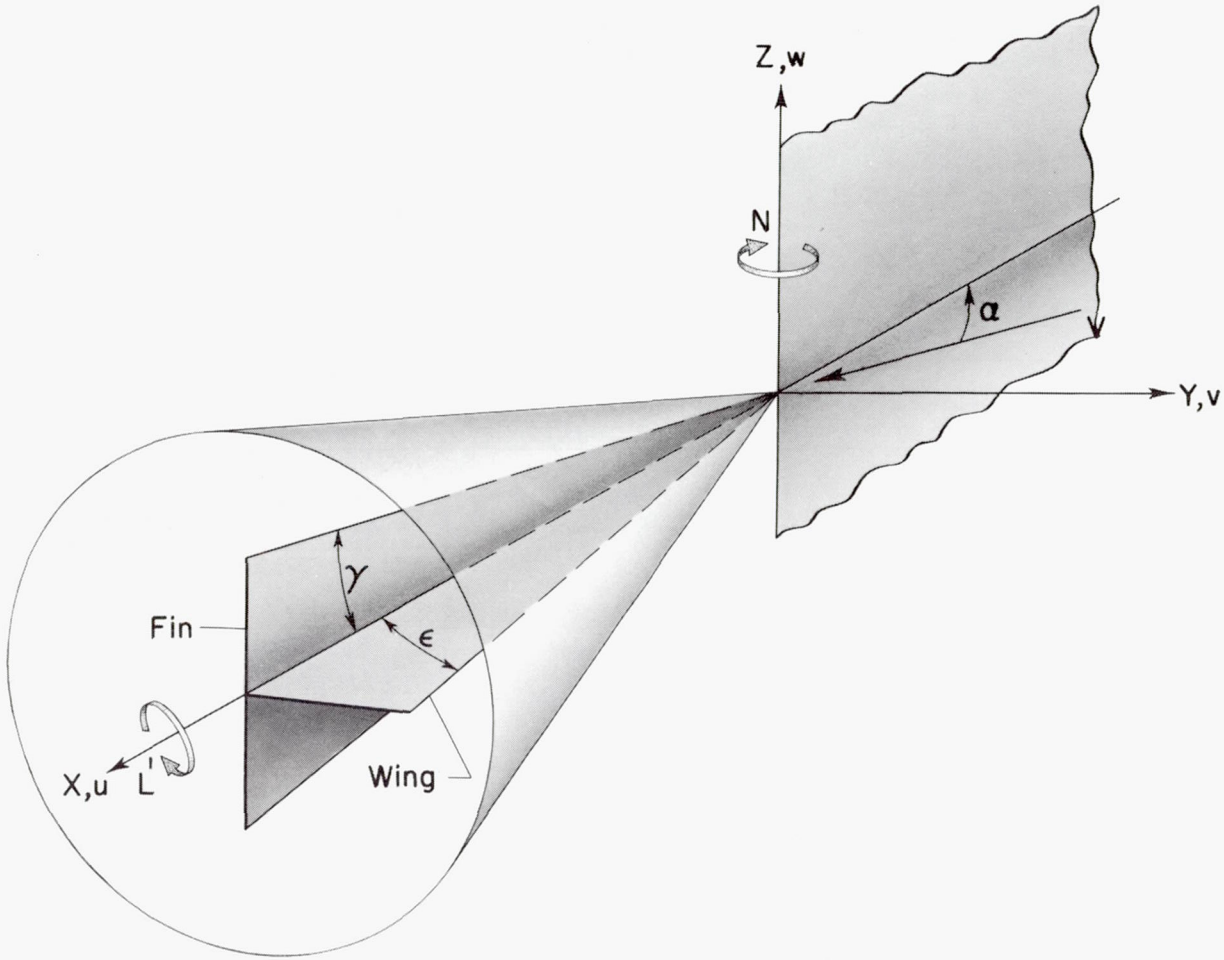

L-81262

Figure 2.- Orientation of tail arrangement for analysis. The horizontal surface, labeled wing, was originally the vertical tail. The vertical surface, labeled fin, was originally the horizontal tail.

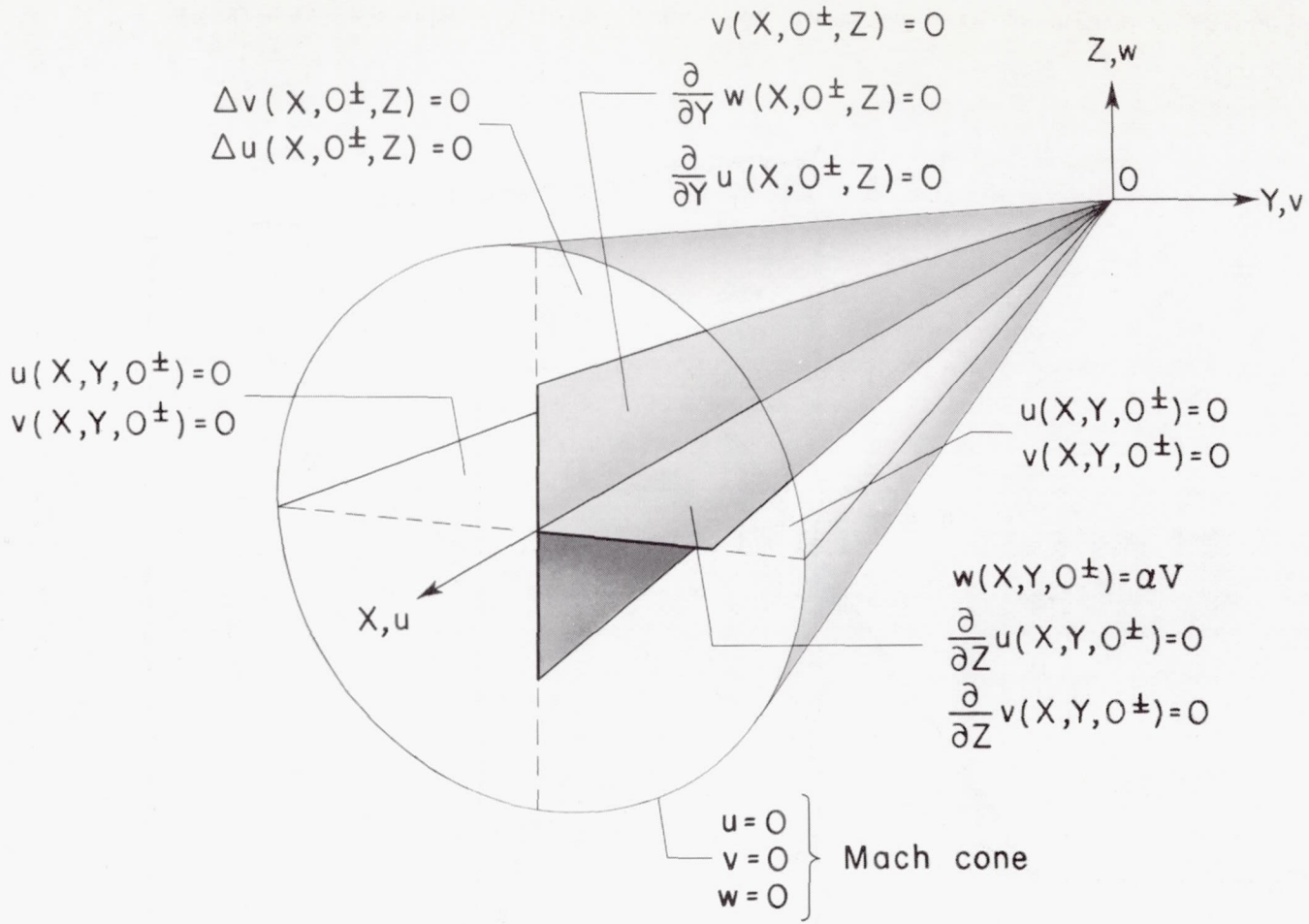

L-81263

Figure 3.- Sketch of wing-fin arrangement showing pertinent values of the u, v, and w disturbance velocities and their spatial derivatives.

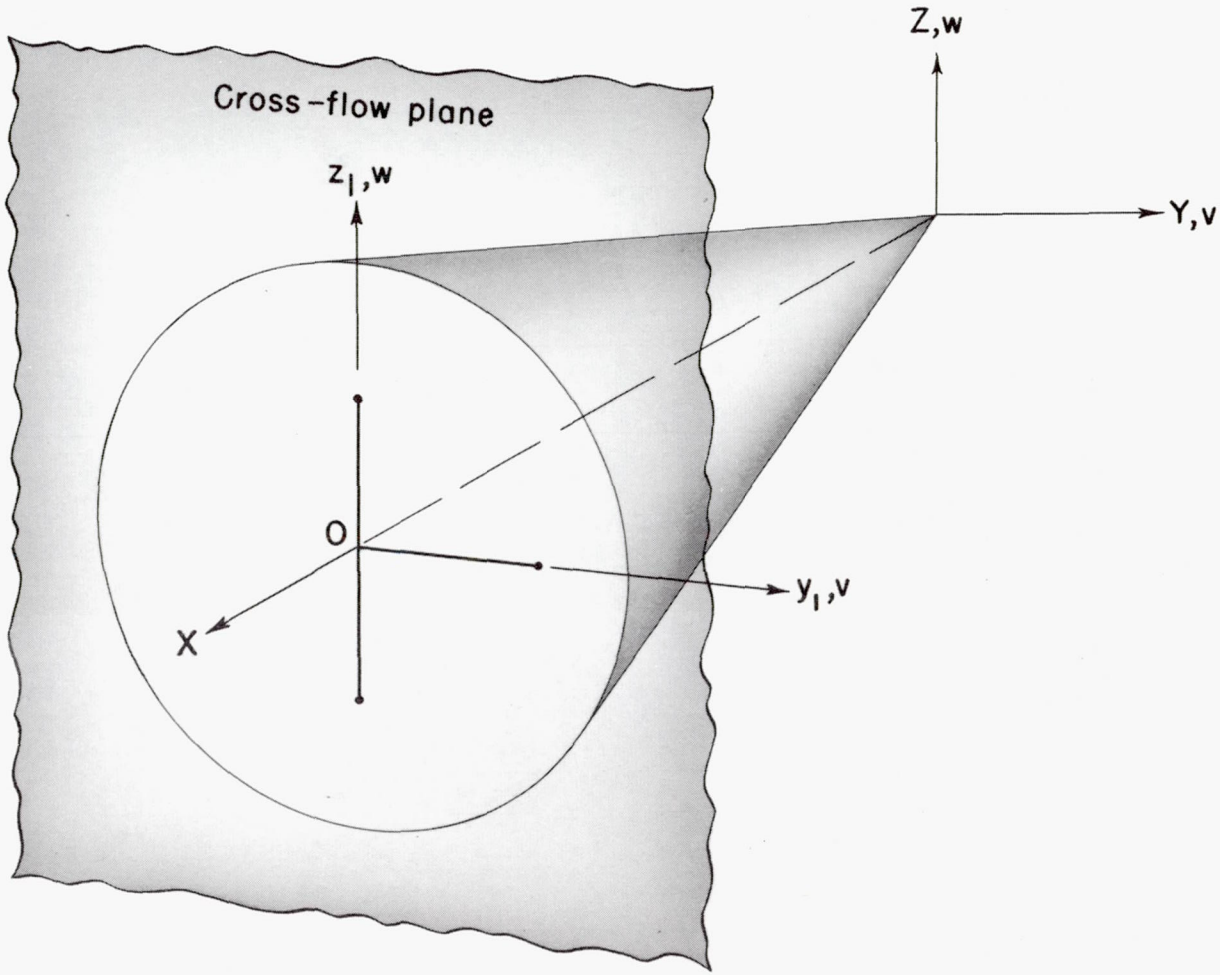

L-81264

Figure 4.- Sketch of typical crossflow plane and its orientation in the X, Y, Z axes system.

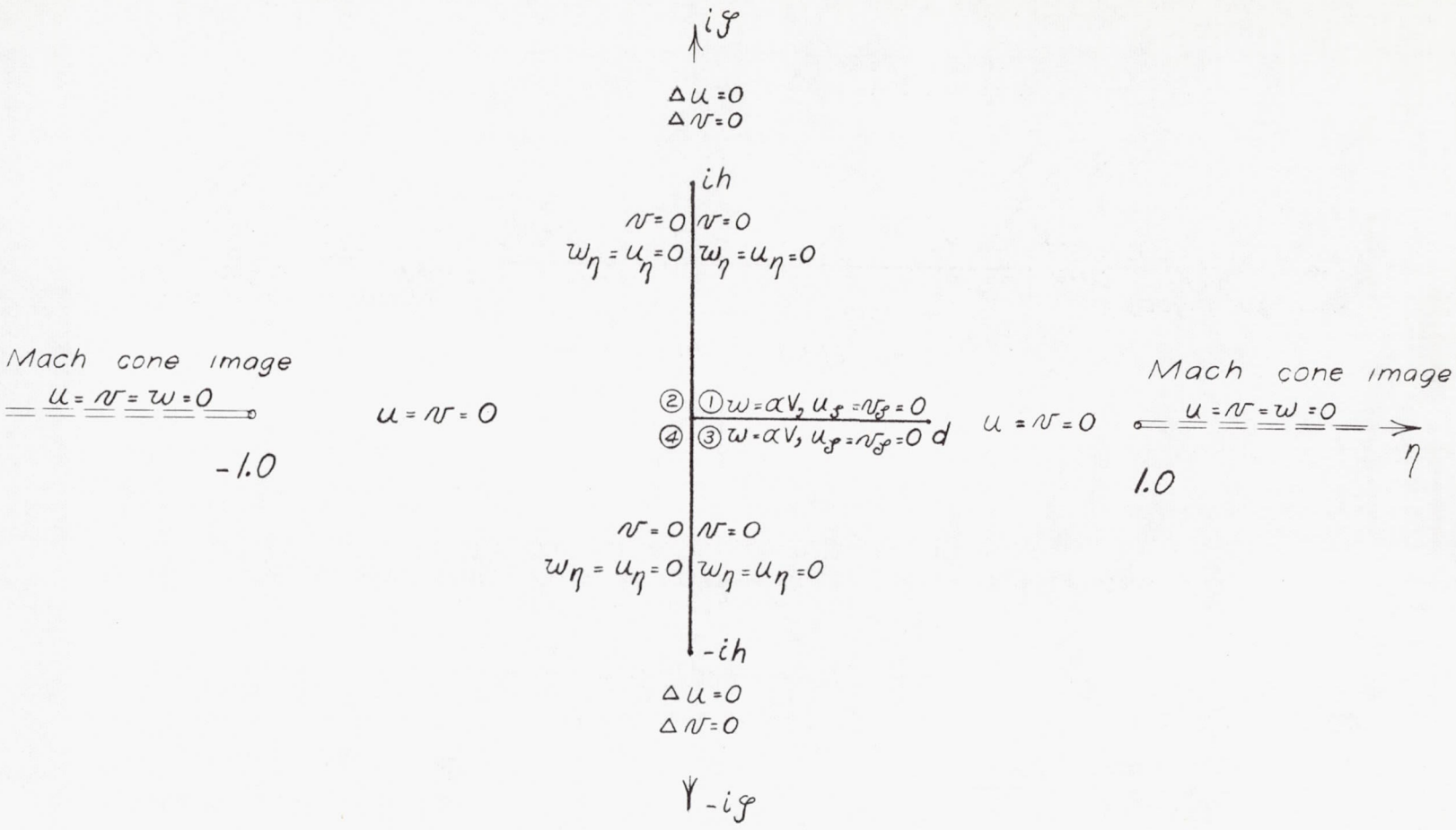

Figure 5.- Sketch of wing-fin arrangement in the $\nu = \eta + i\zeta$ plane showing values of the u-, v-, and w-velocities and their derivatives along the real and imaginary axes.

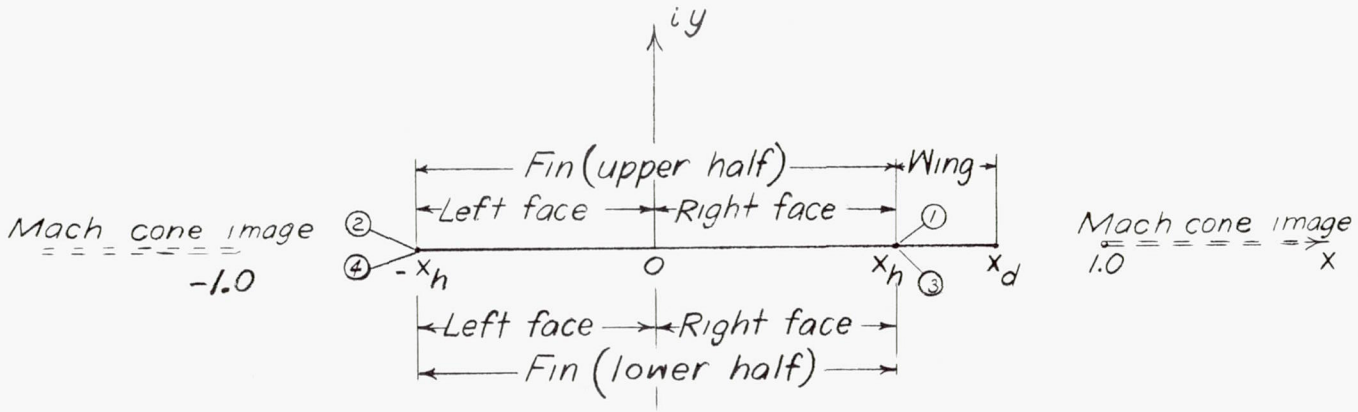

(a) Transformed wing-fin arrangement in the z = x + iy plane.
Numbers refer to numbers in figure 5.

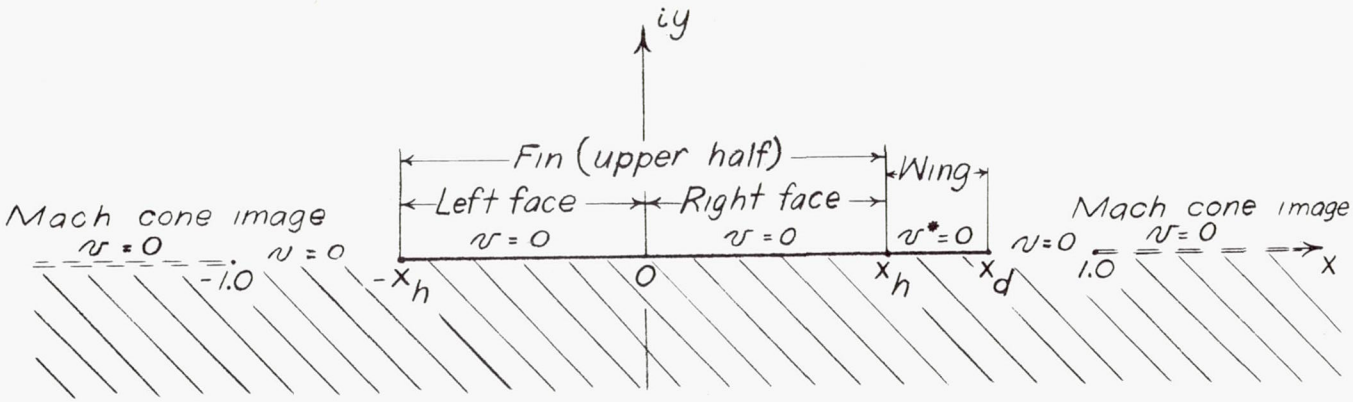

(b) Upper half of z-plane showing boundary values of v and v* along axis of reals.

Figure 6.- Sketch of z-plane including boundary values of v and v* along axis of reals.

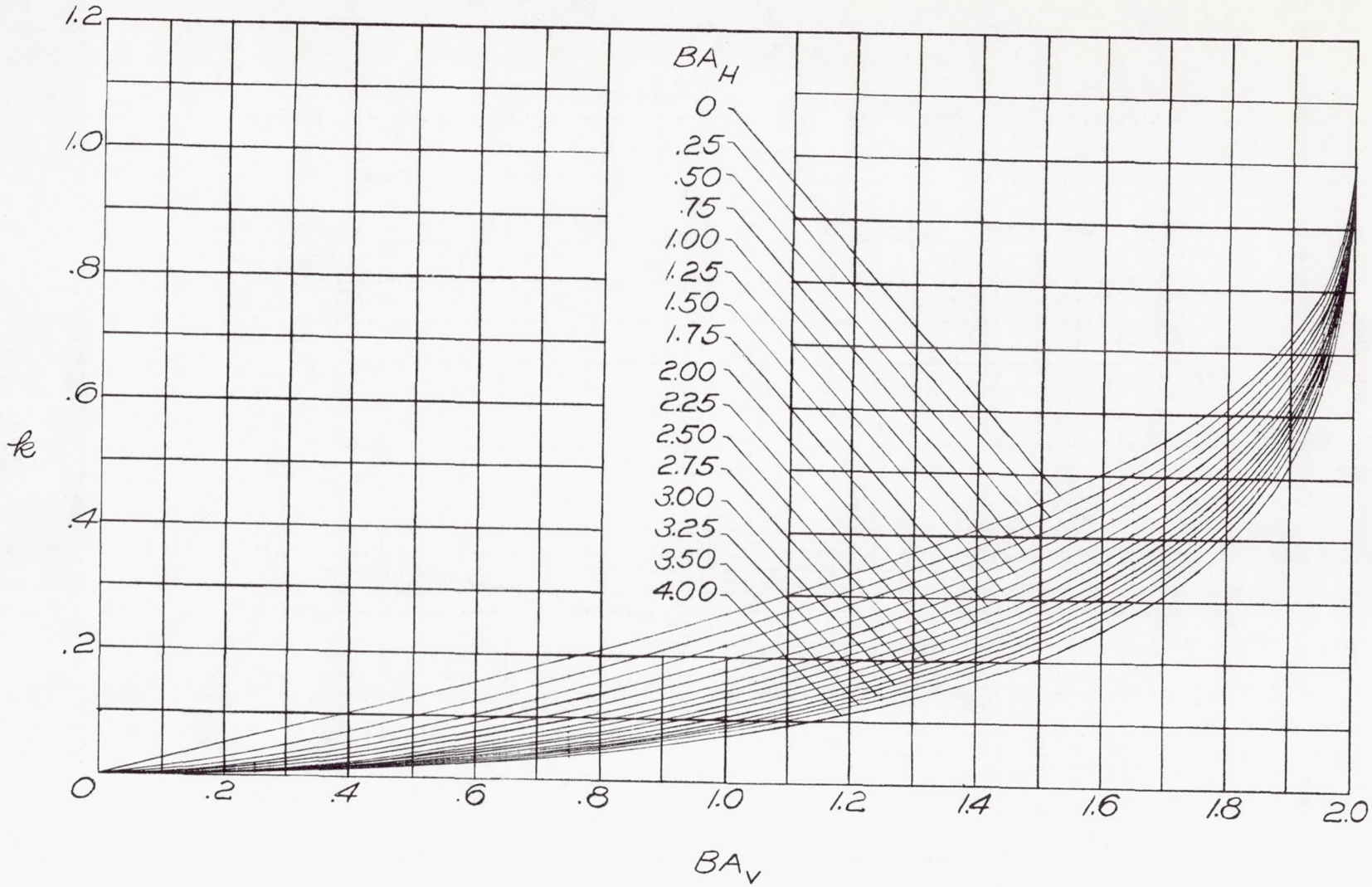

Figure 7.- Variation of k with BA_V for a range of BA_H values.

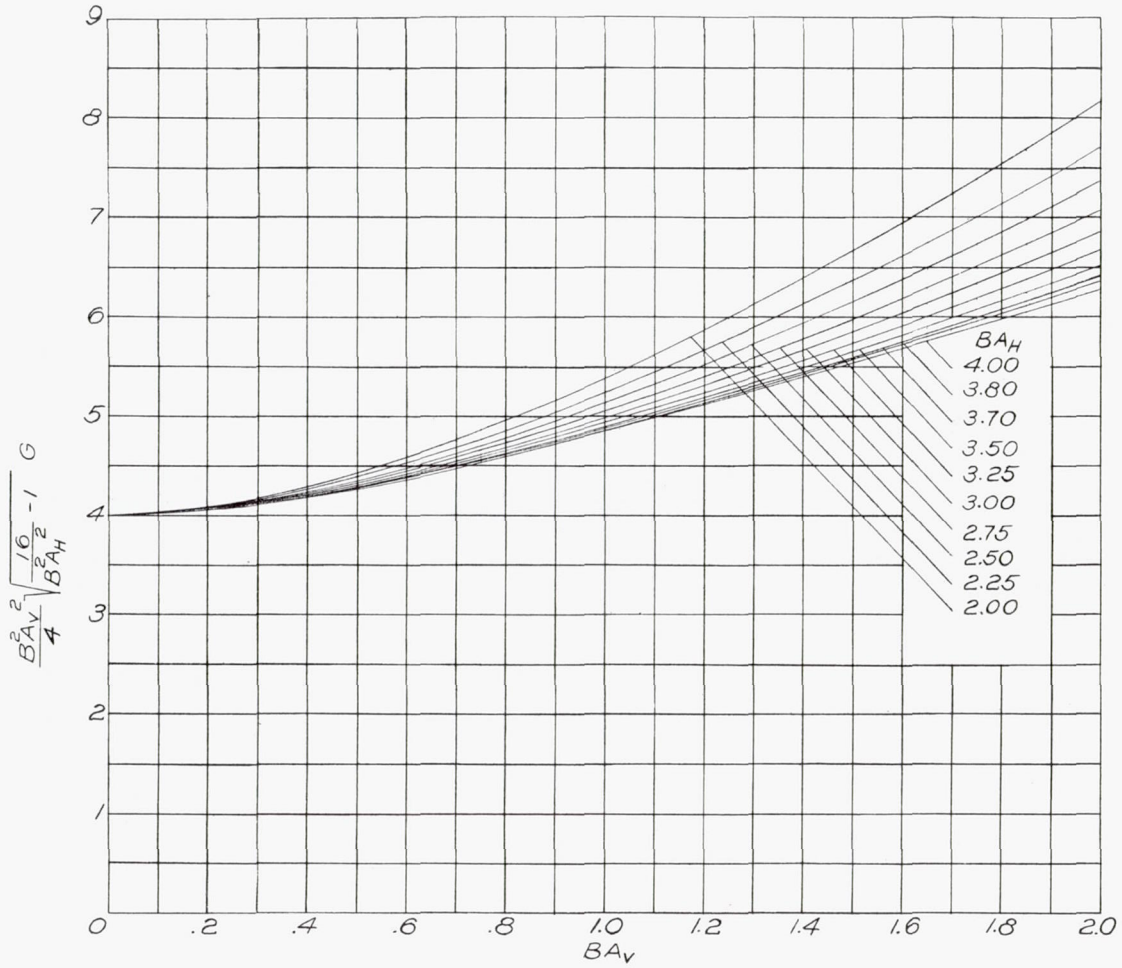

Figure 8.- Variation of $\frac{B^2A_V^2}{4}\sqrt{\frac{16}{B^2A_H^2}-1}\ G$ with BA_V for different values of BA_H.

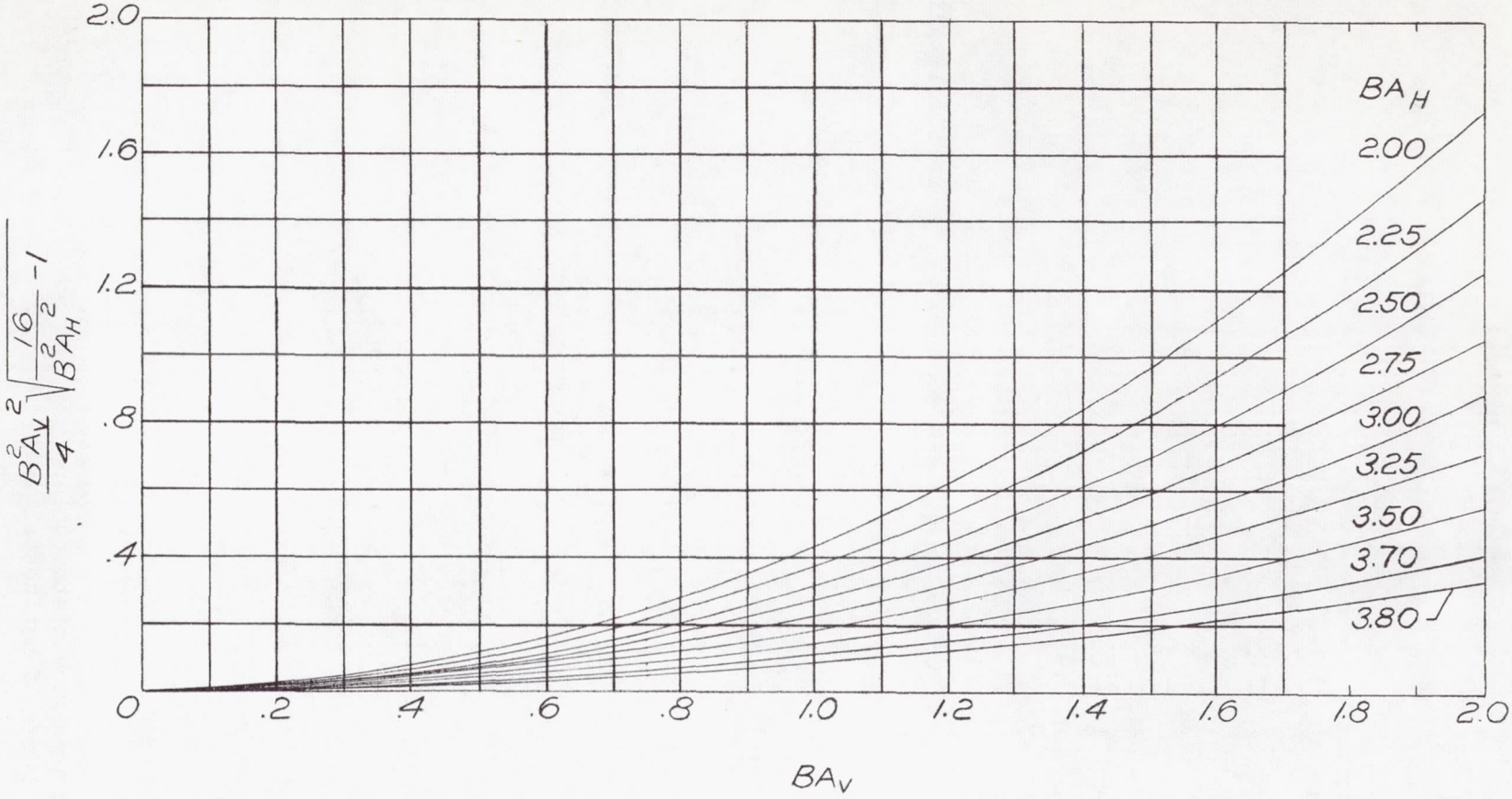

Figure 9.- Variation of $\frac{B^2A_V^2}{4}\sqrt{\frac{16}{B^2A_H^2}-1}$ with BA_V for different values of BA_H.

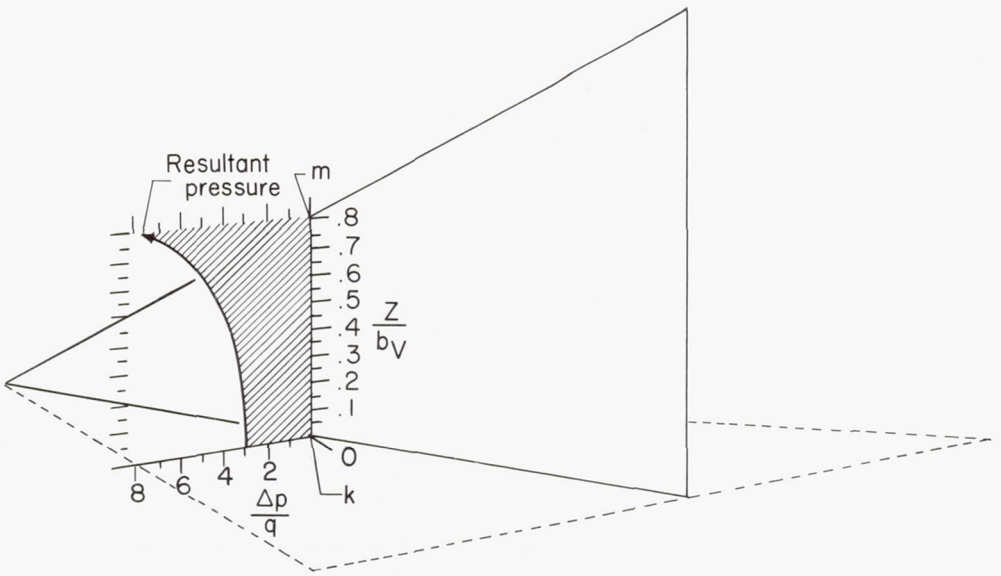

(a) Spanwise pressure distribution along a section k-m of vertical tail.

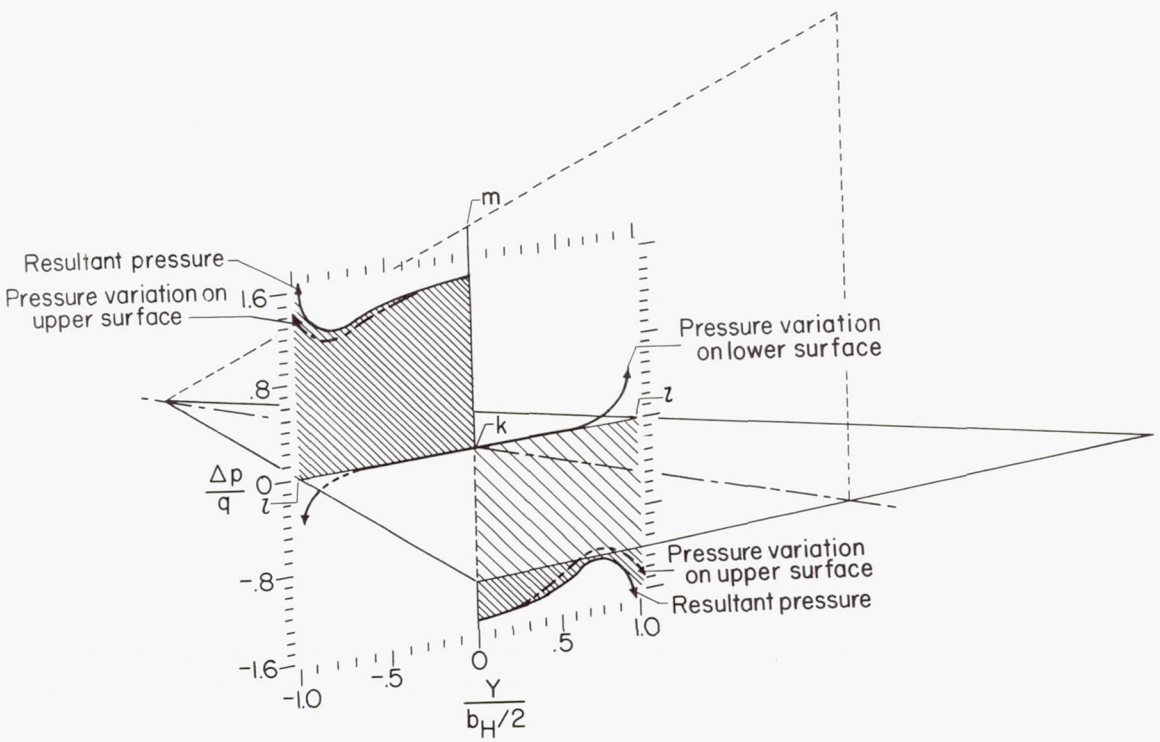

(b) Spanwise pressure distribution along a section l-k-l of horizontal tail.

Figure 10.- Spanwise pressure distributions along section k-m of vertical tail and section l-k-l of horizontal tail. M = 1.17; A_V = 2; A_H = 4.

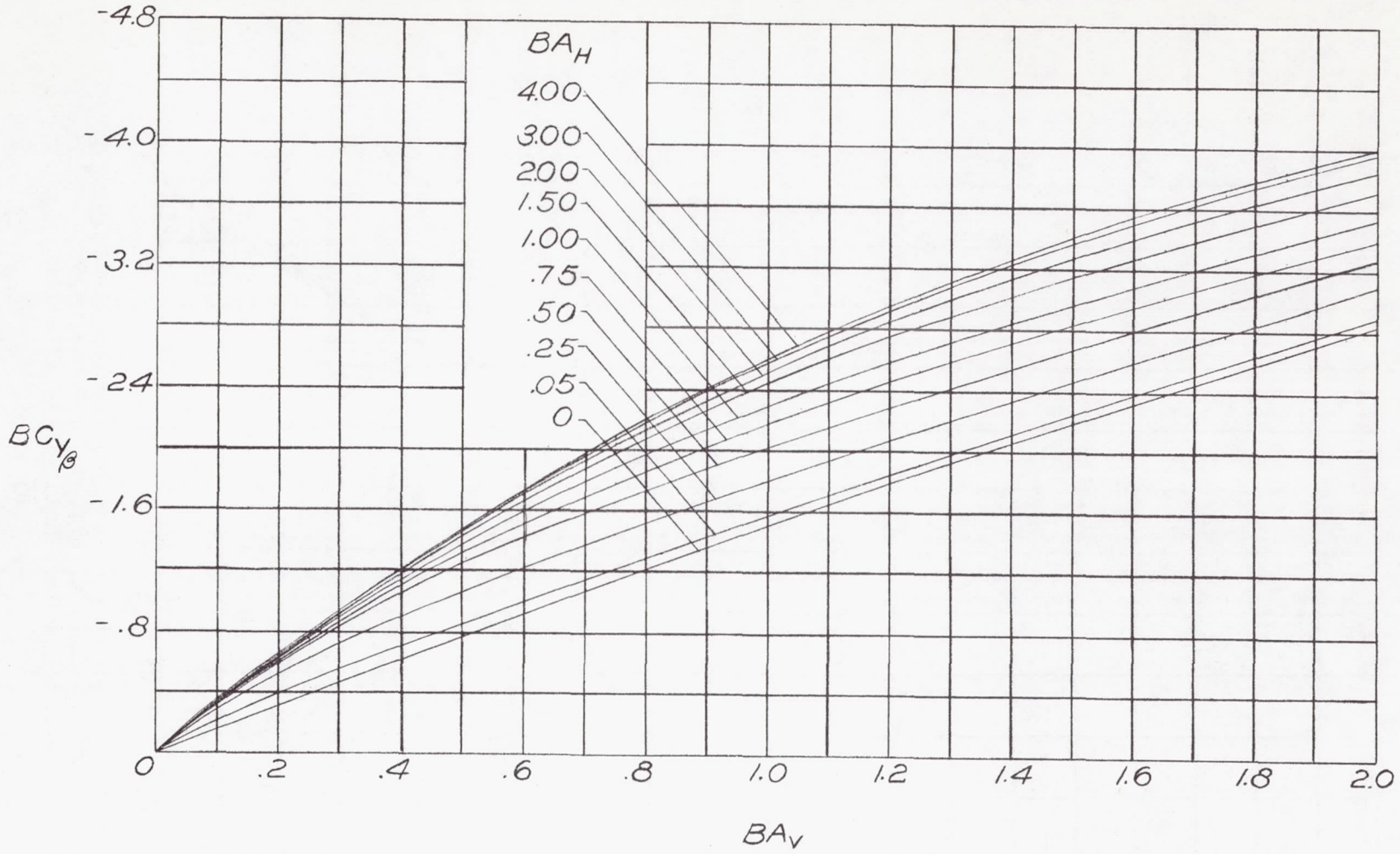

Figure 11.- Variation of BC_{Y_β} with BA_V for various values of BA_H.

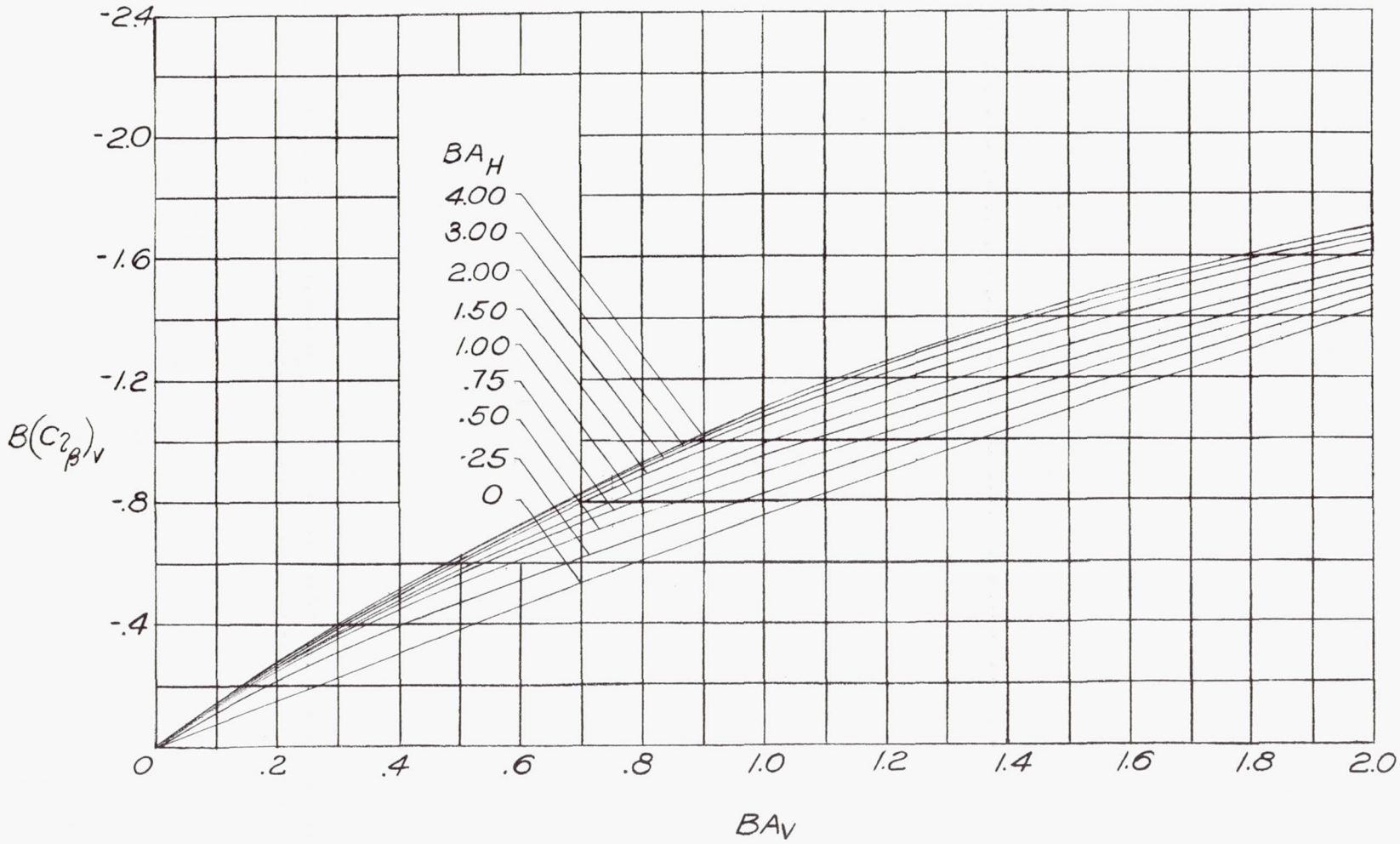

Figure 12.- Variation of $B(C_{l_\beta})_V$ with BA_V for various values of BA_H.

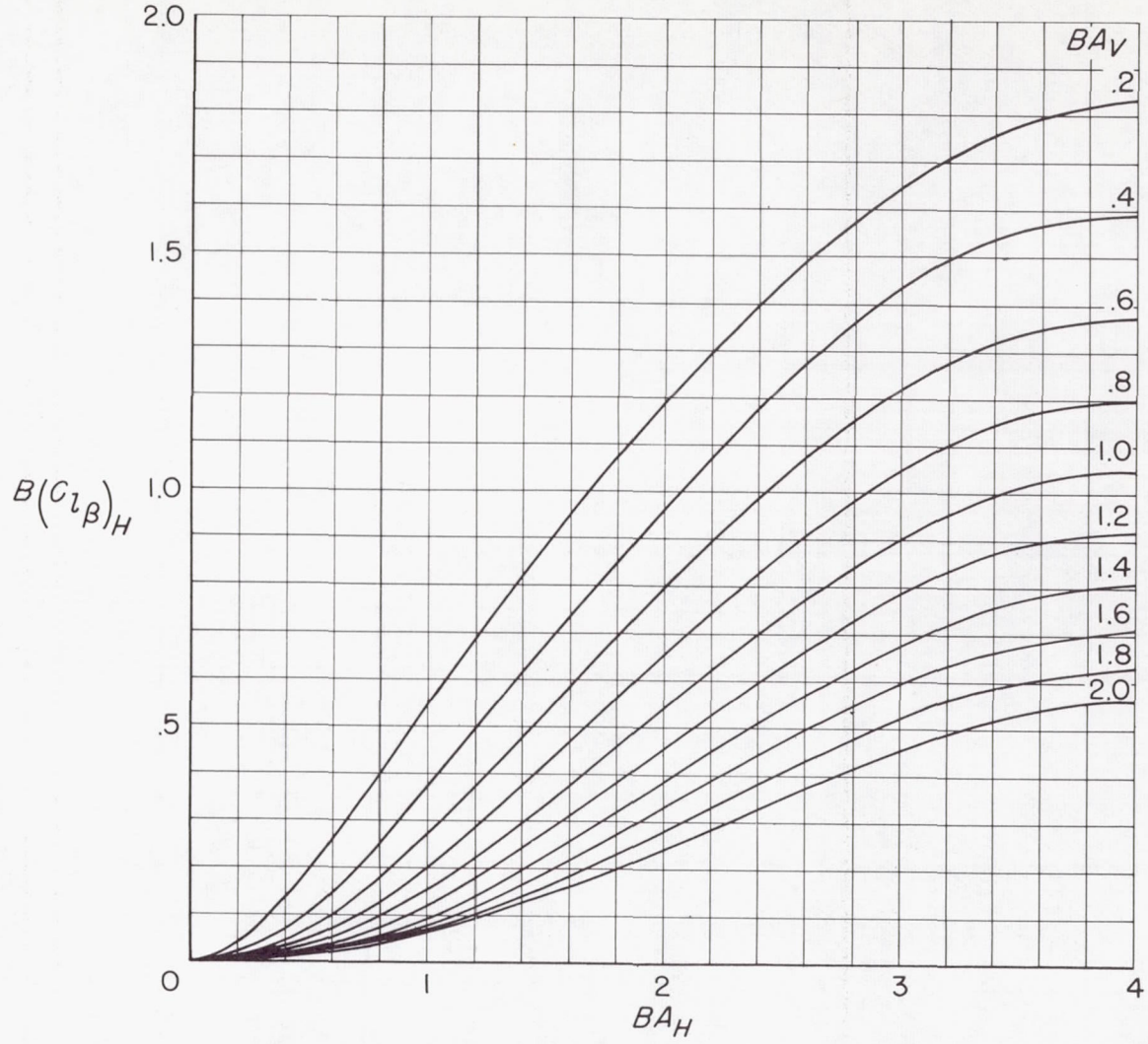

Figure 13.- Variation of $B(C_{l_\beta})_H$ with BA_H for various values of BA_V.

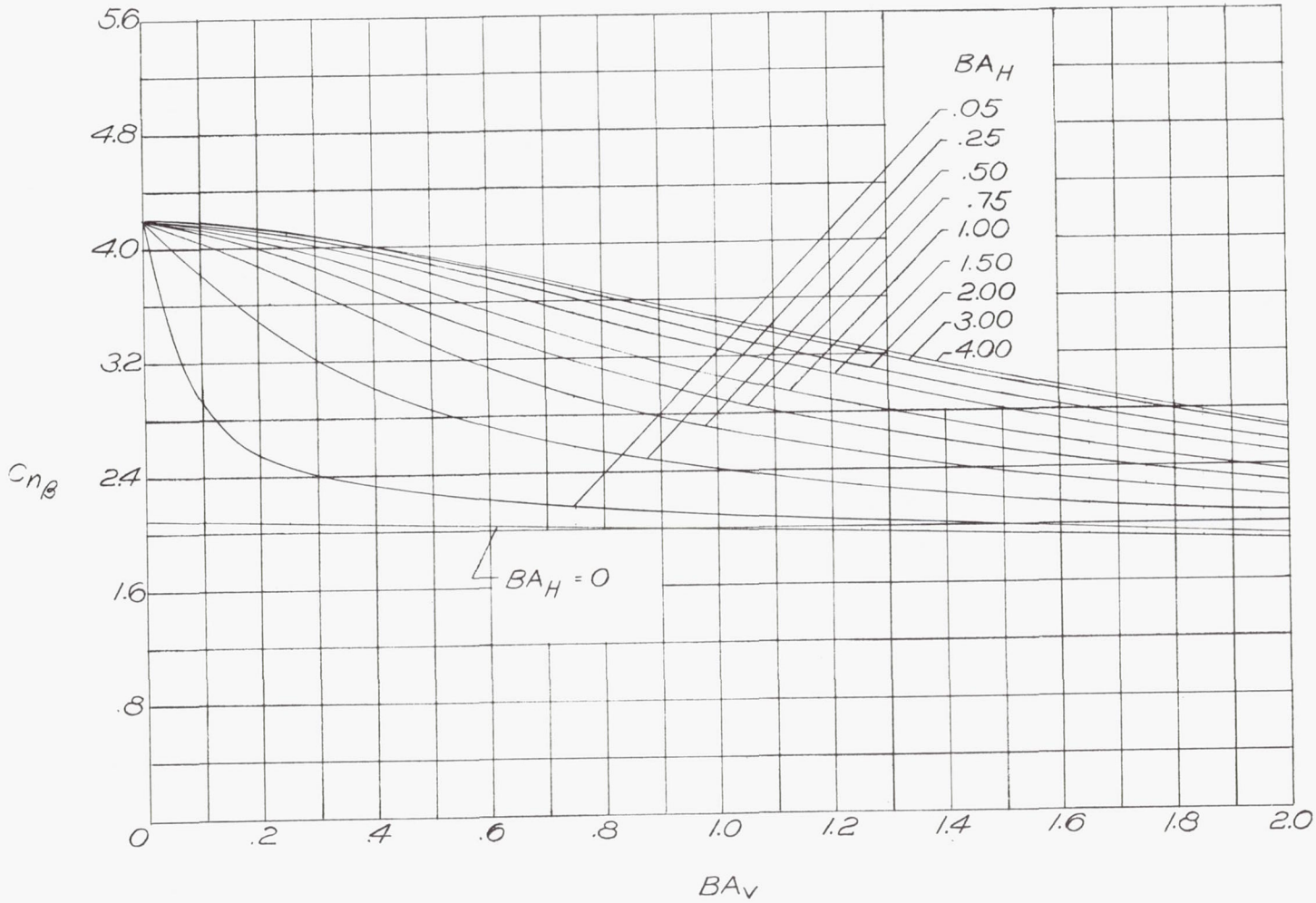

Figure 14.- Variation of C_{n_β} with BA_V for various values of BA_H.
Moment about vertical axis through apex of tail.

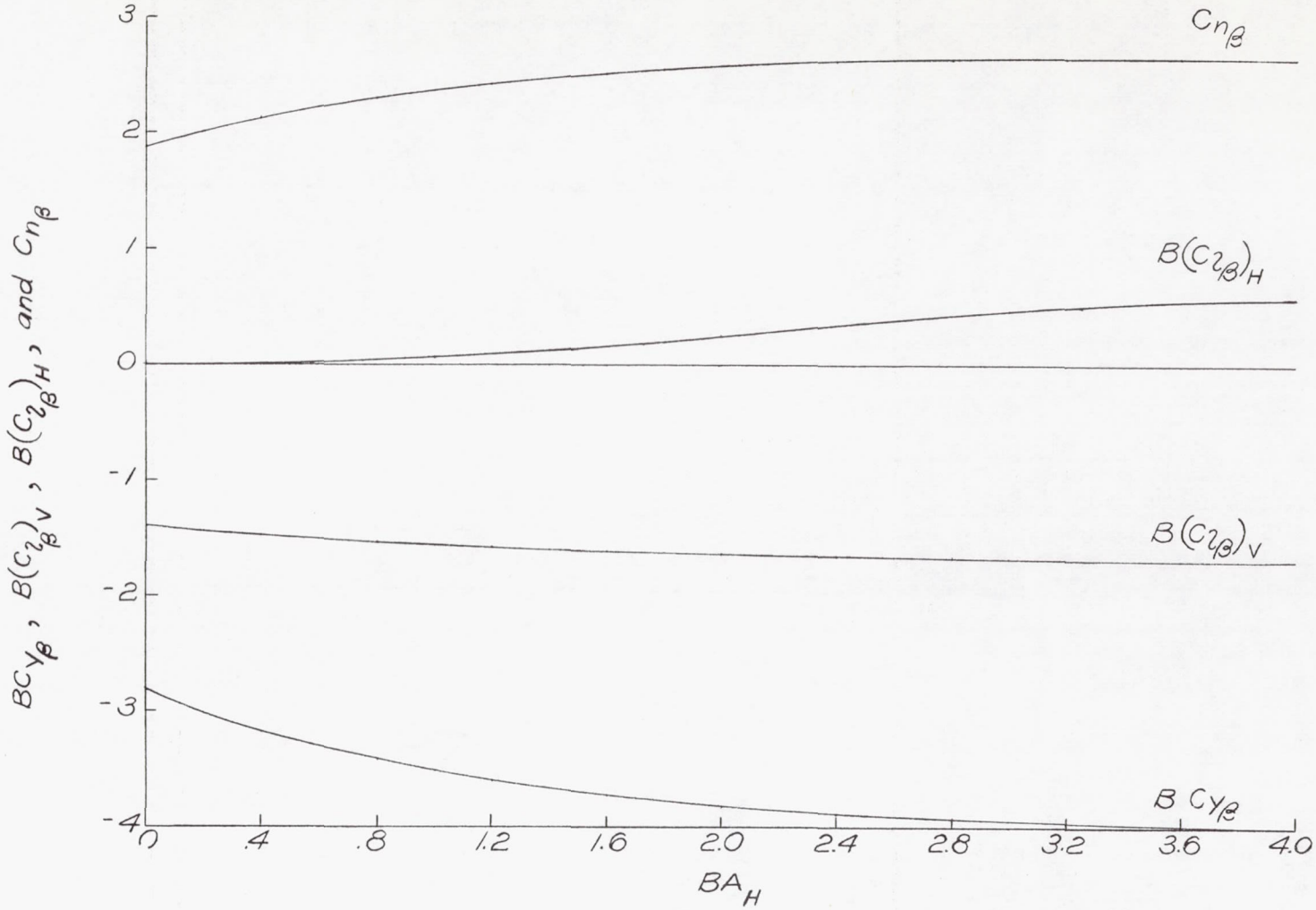

Figure 15.- Variation of BC_{Y_β}, $B\left(C_{l_\beta}\right)_V$, $B\left(C_{l_\beta}\right)_H$, and C_{n_β} with BA_H for $BA_V = 2$ (leading edge of vertical tail is sonic).

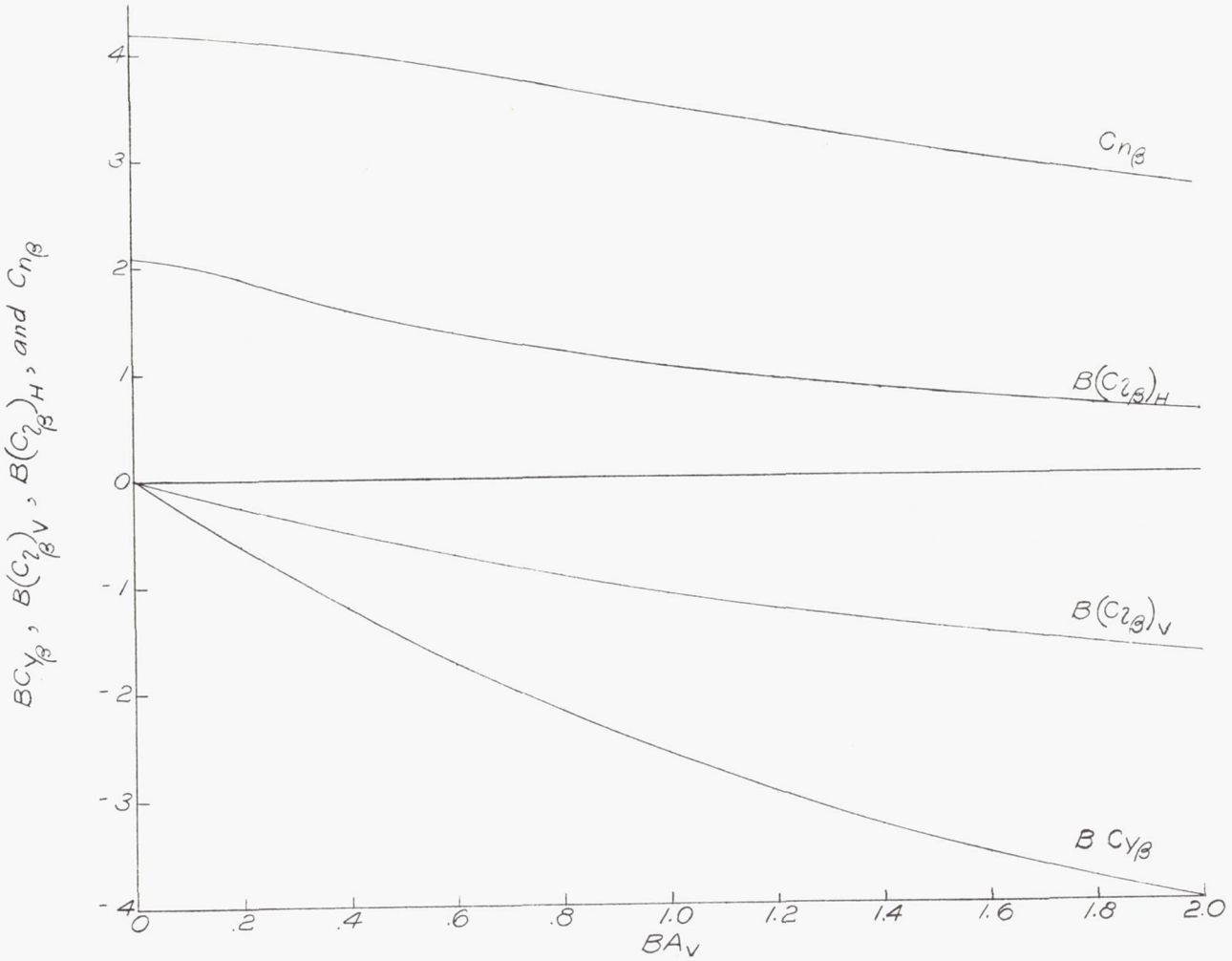

Figure 16.- Variation of BC_{Y_β}, $B\left(C_{l_\beta}\right)_V$, $B\left(C_{l_\beta}\right)_H$, and C_{n_β} with BA_V for $BA_H = 4$ (leading edges of horizontal tail are sonic).

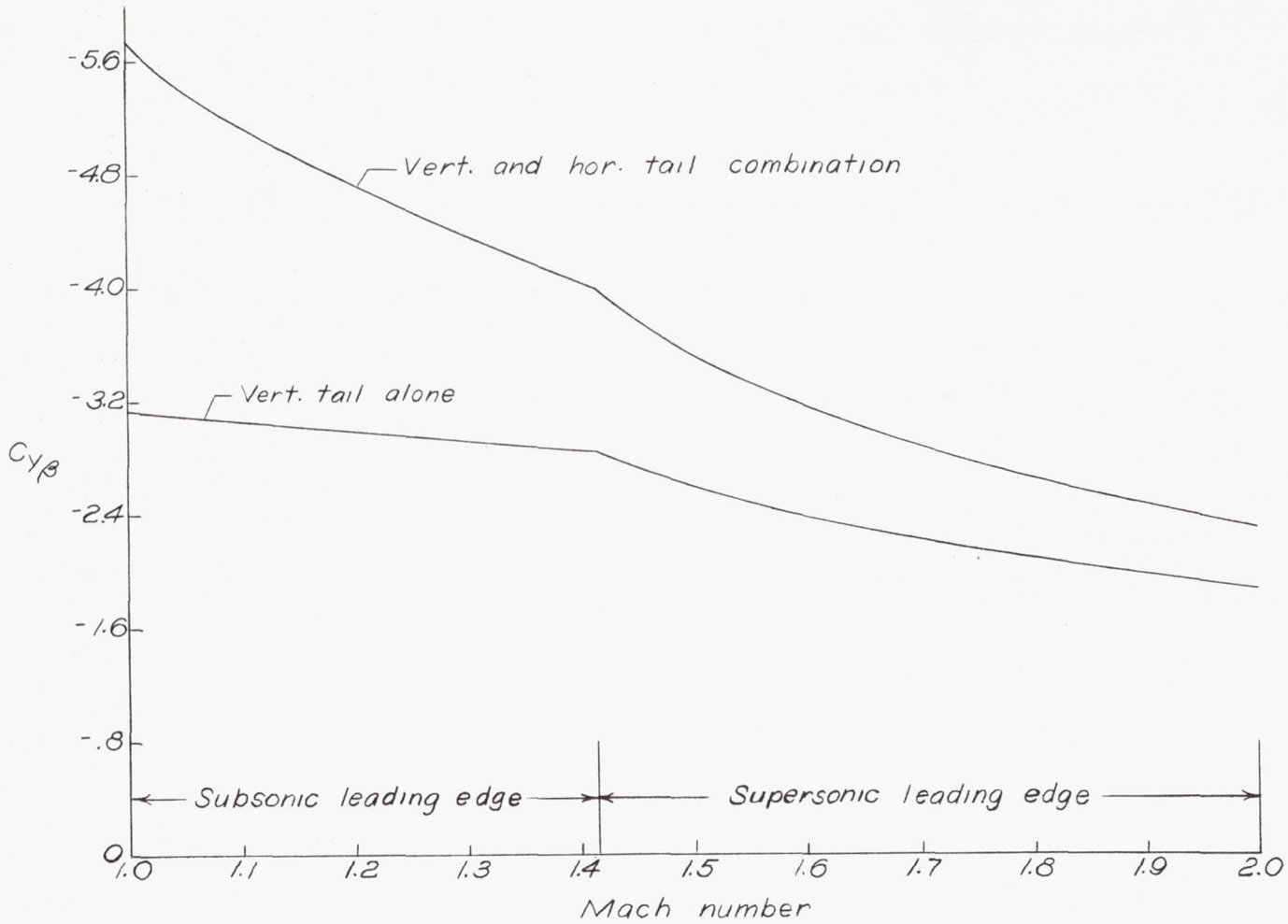

Figure 17.- Illustrative variation of C_{Y_β} with Mach number. $A_V = 2$; $A_H = 4$. Results for supersonic leading edges obtained from reference 4.

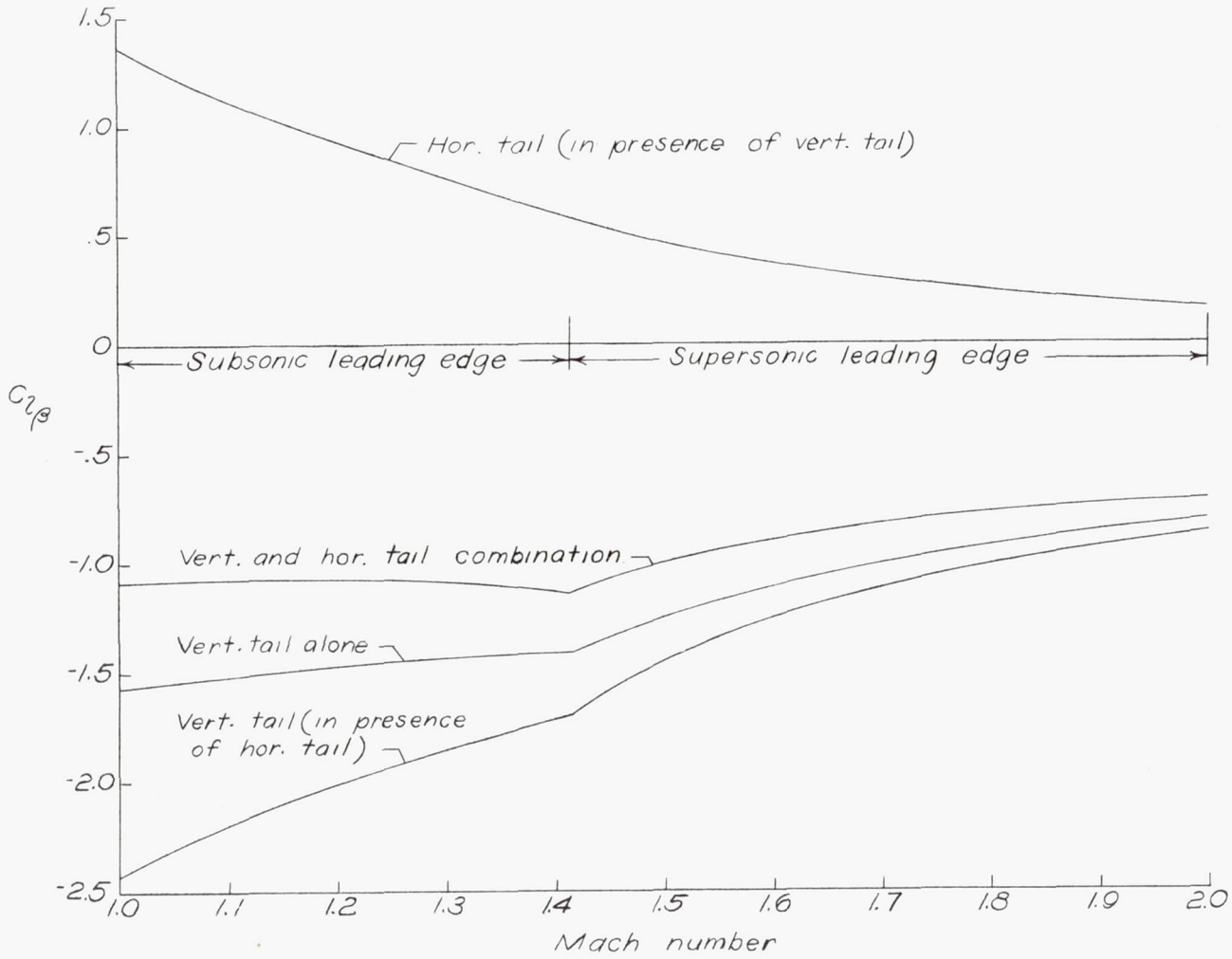

Figure 18.- Illustrative variation of C_{l_β} with Mach number. $A_V = 2$; $A_H = 4$. Results for supersonic leading edges obtained from reference 4.

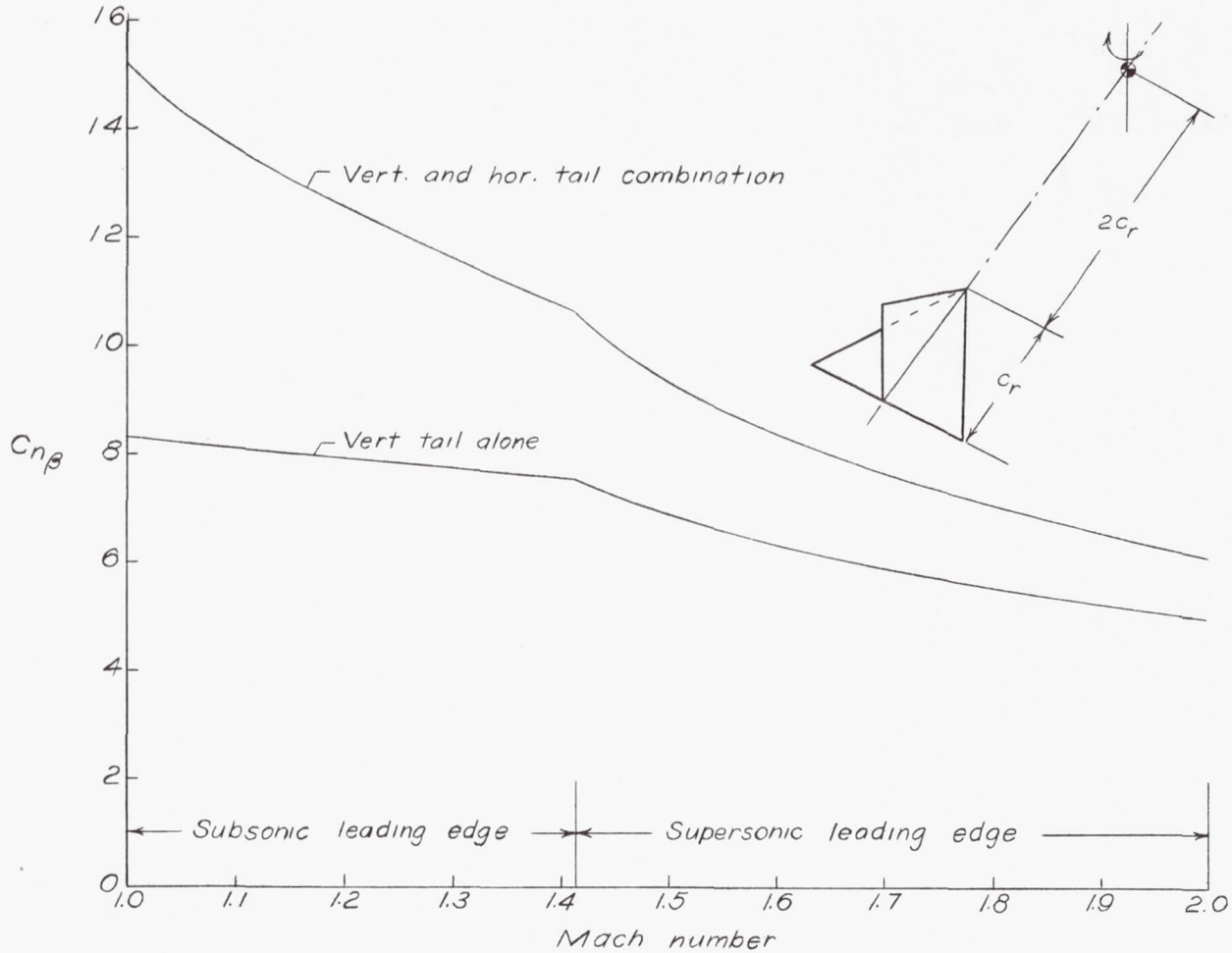

Figure 19.- Illustrative variation of C_{n_β} with Mach number. $A_V = 2$; $A_H = 4$; yawing-moment axis located a distance $2c_r$ ahead of apex of tail. Results for supersonic leading edges obtained from reference 4.

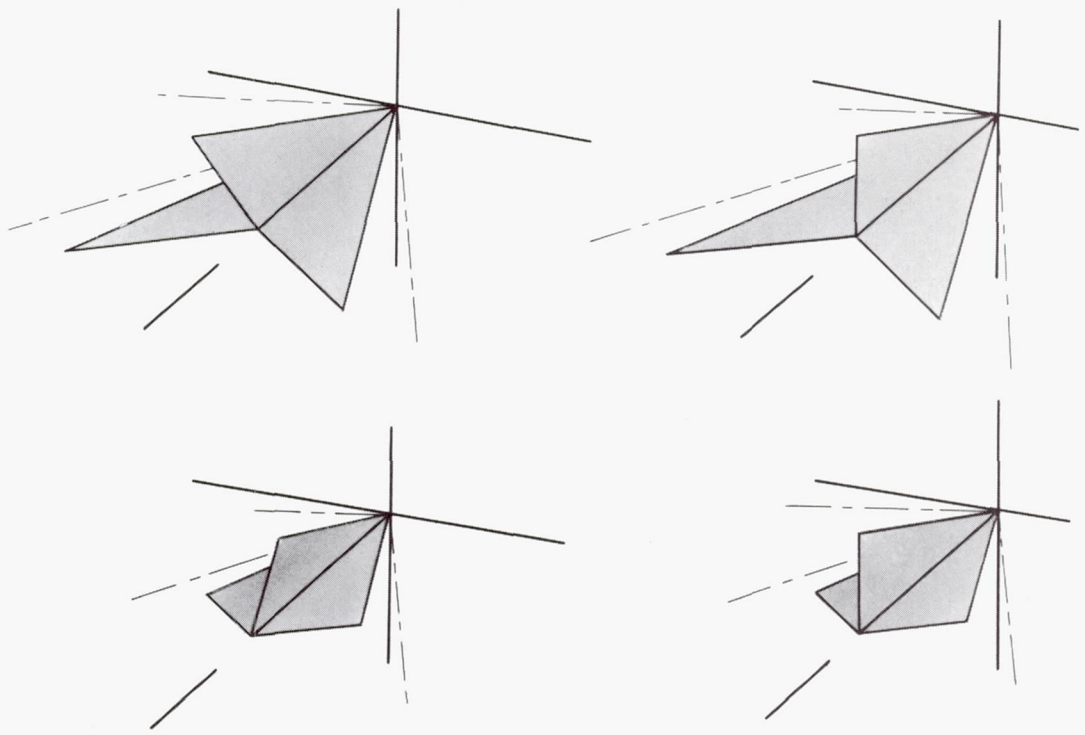

Figure 20.- Plan-form modifications of basic tail surfaces for which the pressure expressions of the basic tail plan forms are also valid.

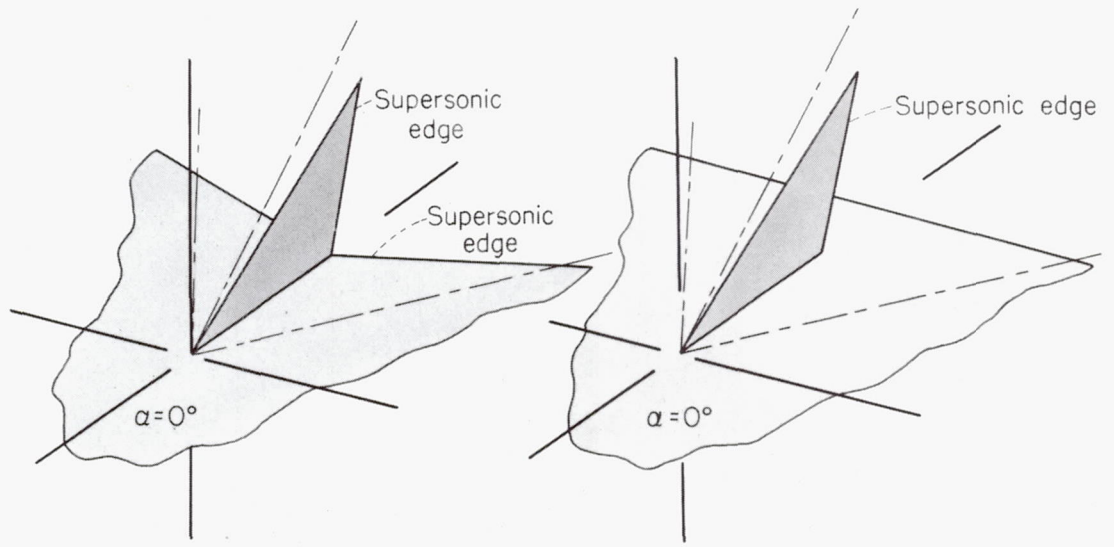

L-81277

Figure 21.- Wing—vertical-tail arrangements for which the pressure expressions of the basic tail plan forms are also valid.

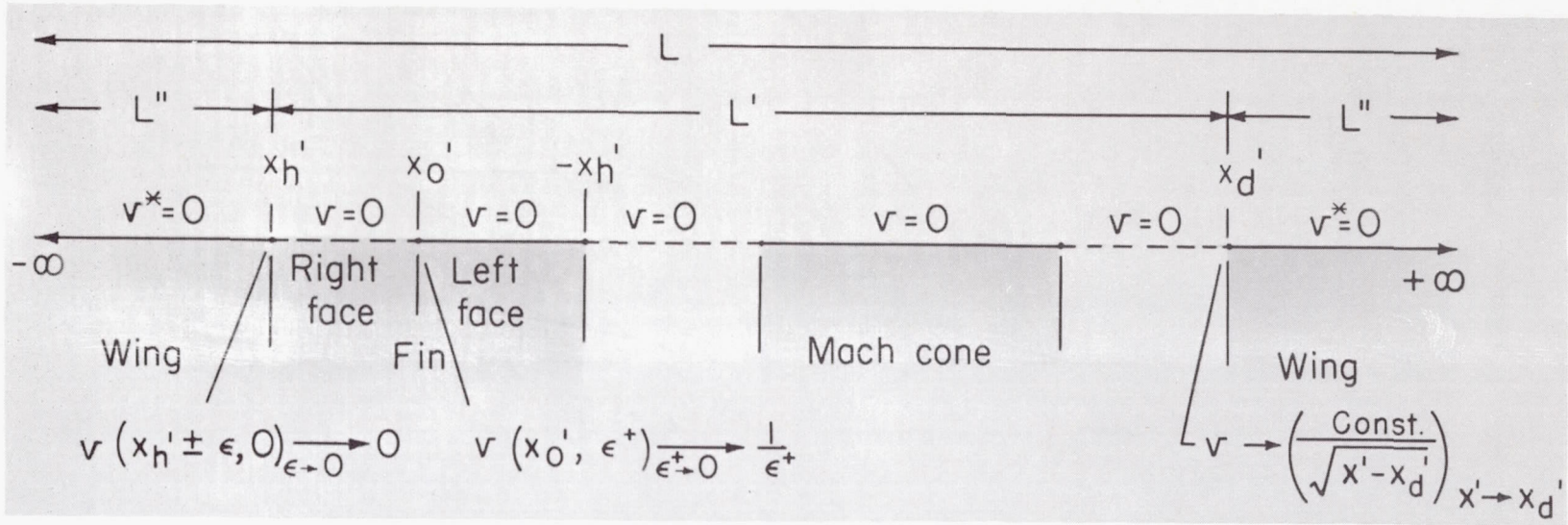

Figure 22.- Sketch of the real axis of z'-plane showing boundary values and singular points of v and v* along real axis. $z' = \dfrac{2}{2z - (x_h + x_d)}$.

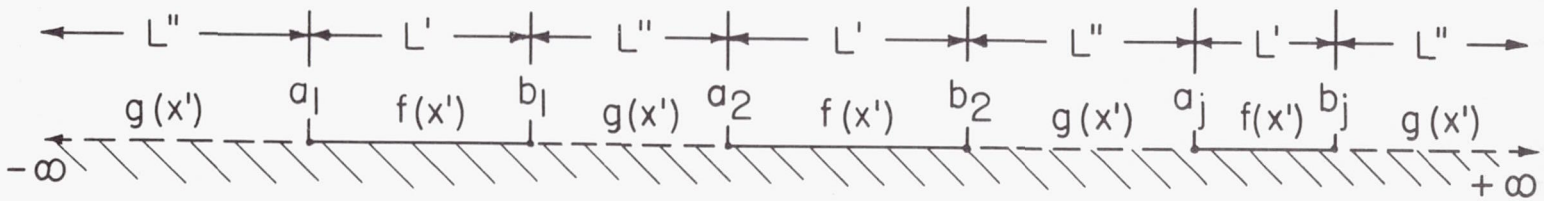

Figure 23.- Notation used in reference 6 in discussion of mixed-type boundary-value problem for the upper half plane.